AD-A164 509 AN EVALUATION OF J-R CURVE TESTING USING THREE POINT BEND SPECIMENS(U) DAVID W TAYLOR NAVAL SHIP RESEARCH AND DEVELOPMENT CENTER ANN.. M T KIRK ET AL. JAN 86 1/1

UNCLASSIFIED DTNSRDC/SME-85/87 F/G 20/11 NL

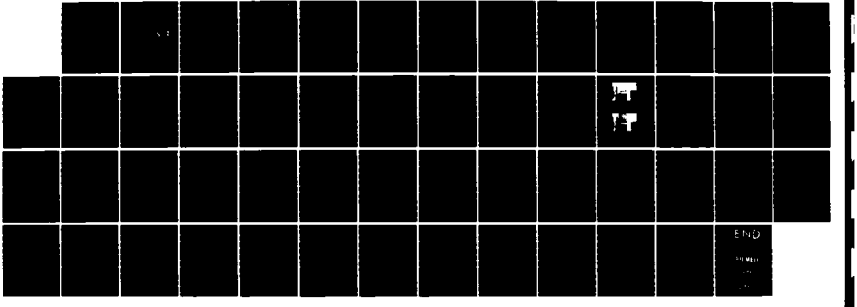

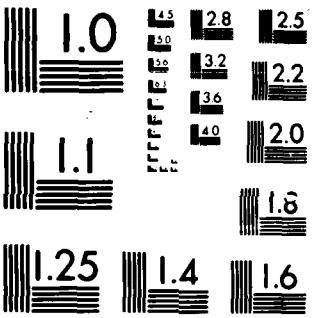


MICROCOPY RESOLUTION TEST CHART

NATIONAL BUREAU OF STANDARDS 1963-A

(12)

DTNSRDC/SME-85/87

# DAVID W. TAYLOR NAVAL SHIP RESEARCH AND DEVELOPMENT CENTER

Bethesda, Maryland 20084

AD-A164 509

## AN EVALUATION OF J-R CURVE TESTING USING THREE POINT BEND SPECIMENS

by

M.T. Kirk

E.M. Hackett



APPROVED FOR PUBLIC RELEASE; DISTRIBUTION UNLIMITED.

SHIP MATERIALS ENGINEERING DEPARTMENT

RESEARCH AND DEVELOPMENT REPORT

January 1986

DTNSRDC/SME-85/87

AN EVALUATION OF J-R CURVE TESTING USING THREE POINT BEND SPECIMENS

## MAJOR DTNSRDC ORGANIZATIONAL COMPONENTS

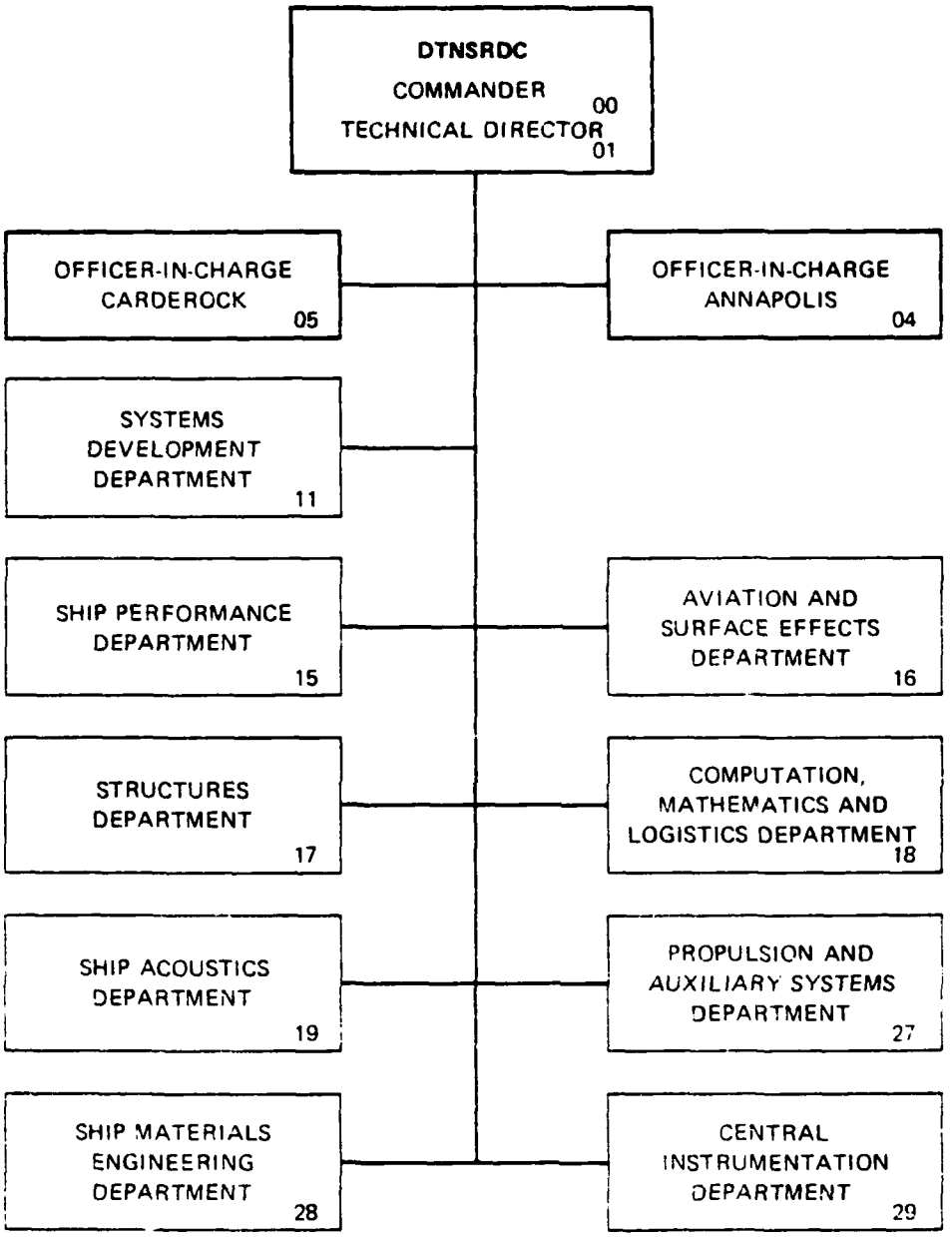

UNCLASSIFIED
SECURITY CLASSIFICATION OF THIS PAGE

AD-A164 509

# REPORT DOCUMENTATION PAGE

| | |
|---|---|
| 1a REPORT SECURITY CLASSIFICATION<br>UNCLASSIFIED | 1b RESTRICTIVE MARKINGS |
| 2a SECURITY CLASSIFICATION AUTHORITY | 3 DISTRIBUTION AVAILABILITY OF REPORT<br>(See reverse side) |
| 2b DECLASSIFICATION / DOWNGRADING SCHEDULE | |
| 4 PERFORMING ORGANIZATION REPORT NUMBER(S)<br>DTNSRDC/SME-85-87 | 5 MONITORING ORGANIZATION REPORT NUMBER(S) |
| 6a NAME OF PERFORMING ORGANIZATION<br>David Taylor Naval Ship R&D Center<br>6b OFFICE SYMBOL (If applicable) | 7a NAME OF MONITORING ORGANIZATION |
| 6c ADDRESS (City, State, and ZIP Code)<br>Bethesda, MD 20084 | 7b ADDRESS (City, State, and ZIP Code) |
| 8a NAME OF FUNDING/SPONSORING ORGANIZATION<br>Naval Sea Systems Command<br>8b OFFICE SYMBOL (If applicable)<br>SEA 05R25 | 9 PROCUREMENT INSTRUMENT IDENTIFICATION NUMBER |
| 8c ADDRESS (City, State, and ZIP Code)<br>Washington, D.C. 20362 | 10 SOURCE OF FUNDING NUMBERS<br>PROGRAM ELEMENT NO: 6276W<br>PROJECT NO:<br>TASK NO:<br>WORK UNIT ACCESSION NO: 1-2814-210-6[illegible] |

11 TITLE (Include Security Classification)
An Evaluation of J-R Curve Testing Using Three Point Bend Specimens

12 PERSONAL AUTHOR(S)
M.T. Kirk and E.M. Hackett

| 13a TYPE OF REPORT | 13b TIME COVERED | 14 DATE OF REPORT (Year, Month, Day) | 15 PAGE COUNT |
|---|---|---|---|
| Research & Development | FROM _____ TO _____ | January 1986 | 51 |

16 SUPPLEMENTARY NOTATION

| 17 COSATI CODES | | | 18 SUBJECT TERMS (Continue on reverse if necessary and identify by block number) |
|---|---|---|---|
| FIELD | GROUP | SUB-GROUP | J-R Curve Testing, Three Point Bend Specimens, Load Line Deflection Measurements |
| | | | |
| | | | |

19 ABSTRACT (Continue on reverse if necessary and identify by block number)

This investigation concerns the accuracy of load line deflection measurement techniques used in J integral-R curve testing of three point bend specimens. Four methods of load line deflection measurement were investigated. One method employed a calibrated transducer that gave a direct reading of load line deflection. The other three methods mathematically related load line deflection to some other displacement (i.e. crack mouth opening displacement, cross head displacement) measured during testing. Photographs taken at regular intervals during loading provided an absolute measure of load line deflection. In comparison to this reference, the other methods had equal accuracy with varying degrees of precision. In no case, however, did the measurements from the laboratory techniques deviate from the photographic reference by more than 0.052 mm (0.002 in.) on average. The small differences between the load line deflections measured by the various laboratory techniques cause less scatter in the J-R curves and $J_{Ic}$ values than attributable to material

(Continued on reverse side)

| 20 DISTRIBUTION/AVAILABILITY OF ABSTRACT | 21 ABSTRACT SECURITY CLASSIFICATION |
|---|---|
| ☐ UNCLASSIFIED/UNLIMITED ☒ SAME AS RPT ☐ DTIC USERS | Unclassified |
| 22a NAME OF RESPONSIBLE INDIVIDUAL<br>M. T. Kirk | 22b TELEPHONE (Include Area Code)<br>(301)267-2368<br>22c OFFICE SYMBOL<br>2814 |

DD FORM 1473, 84 MAR 83 APR edition may be used until exhausted
All other editions are obsolete

SECURITY CLASSIFICATION OF THIS PAGE

☆U.S. Government Printing Office: 1985—520-012

Block 3

APPROVED FOR PUBLIC RELEASE; DISTRIBUTION UNLIMITED.

Block 19 continued

variability. Further, J-R curves over the first 1.75 mm of crack extension from both bendbars and compacts were shown to be coincident for the alloys tested.

TABLE OF CONTENTS


| | Page |
|---|---|
| LIST OF FIGURES | iii |
| LIST OF TABLES | v |
| LIST OF ABBREVIATIONS | vi |
| ABSTRACT | 1 |
| ADMINISTRATIVE INFORMATION | 1 |
| INTRODUCTION | 1 |
| EXPERIMENTAL PROCEDURE | 3 |
| MATERIAL AND TEST SPECIMENS | 3 |
| THREE POINT BEND TESTING | 4 |
| COMPACT TENSION TESTING | 4 |
| LOAD LINE DEFLECTION MEASUREMENTS | 4 |
| MEASURED FROM PHOTOGRAPHS | 4 |
| MEASURED FROM FLEX BAR TRANSDUCER | 6 |
| CALCULATED FROM CROSS HEAD DISPLACEMENT | 6 |
| CALCULATED FROM CLIP GAGE MEASUREMENTS | 6 |
| RESULTS AND DISCUSSION | 8 |
| SUMMARY | 11 |
| REFERENCES | 43 |


LIST OF FIGURES


| | |
|---|---|
| 1 - Diagrams of Specimens Tested | 12 |
| 2 - Schematic of Computer Interactive Test Apparatus | 13 |
| 3 - Schematic of Flex Bar and Its Attachment to Three Point Bend Specimen | 14 |
| 4 - Procedure for Determination of Load Line Displacement from Photographs | 15 |

Page

5 - Diagram Showing Terms Used in Equations Based on Rigid Rotation Assumptions . . . . . 16

6 - Expected Error in Load Line Displacement Measurements from the Photographs Due to Limited Digitizing Pad Resolution and Horizontal Reference Bar Motion . . . . . 17

7 - Load Versus Testing Machine Cross Head Displacment Characteristic . . . 18

8 - Relation Between Load Line Deflection and $d_{CMOD}$ Determined Using Rigid Rotation Assumptions . . . . . 19

9 - Relation Between Load Line Deflection and $d_{CMOD}$ Determined Using Empirical Correlation . . . . . 20

10 - Load Versus Load Line Deflection Determined Using Various Experimental Techniques Compared to the Photographic Data (A-710 Specimen GES-40) . . . . . 21

11 - Load Versus Load Line Deflection Determined Using Various Experimental Techniques Compared to the Photographic Data (3-Ni Specimen FYB-503 . . . . . 26

12 - Comparison of Load Line Deflection Measured Using Various Experimental Techniques to the Photographic Load Line Deflection Measurements for all Specimens Tested . . . . . 30

13 - Plot Showing the Acceptable Data Region and the Residual of a Data Point Lying Outside of the Region . . . . . 35

14 - J-R Curves for Three Bendbars Showing the Effect of Different Load Line Deflection Measurments and Material Scatter. . . . . 36

15 - Comparison of J-R Curves Determined Using Bendbars to J-R Curves Determined Using Compact Tension Specimens of the Same Material . . . . . 39

LIST OF TABLES


| | Page |
|---|---|
| 1 - Chemical and Mechanical Property Data . . . . . | 3 |
| 2 - Empirical Correlation Slopes Relating Load Line Displacement to Crack Mouth Opening Displacement . . . . . | 7 |
| 3 - Least Squares Coefficients for Comparisons of Deflection Measurements to Photographic Reference . . . . . | 8 |
| 4 - Average Residuals of Each Measurement Technique From the Photographic Reference . . . . . | 9 |
| 5 - $J_{Ic}$ Values . . . . . | 10 |

## LIST OF ABBREVIATIONS

| | |
|---|---|
| $b$ | Uncracked ligament |
| $\beta$ | Empirical coefficient expressing fraction of b around which the remaining ligament is assumed to hinge |
| $E$ | Young's modulus |
| $I$ | Moment of inertia |
| $d_{CMOD}$ | Crack mouth opening displacement |
| $D_{LL}$ | Load line deflection |
| $D_{LL}^{d}$ | Load line deflection calculated using $d_{CMOD}$ |
| $D_{LL}^{drc}$ | Load line deflection calculated using $d_{CMOD}$ with a rotation correction |
| $D_{LL}^{corr}$ | Load line deflection calculated using an experimentally developed correlation |
| $h_o$ | Original height of the horizontal reference bar support point above the roller |
| $J_{IC}$ | Mode I critical fracture toughness |
| $m$ | Slope of a plot of $D_{LL}$ versus $d_{CMOD}$ |
| $P$ | Load |
| $S$ | Span between rollers |
| $W$ | Specimen width |

## ABSTRACT

This investigation concerns the accuracy of load line deflection measurement techniques used in J integral-R curve testing of three point bend specimens. Four methods of load line deflection measurement were investigated. One method employed a calibrated transducer that gave a direct reading of load line deflection. The other three methods mathematically related load line deflection to some other displacement (i.e. crack mouth opening displacment, cross head displacment) measured during testing. Photographs taken at regular intervals during loading provided an absolute measure of load line deflection. In comparison to this reference, the other methods had equal accuracy with varying degrees of precision. In no case, however, did the measurements from the laboratory techniques deviate from the photographic reference by more than 0.052 mm (0.002 in.) on average. The small differences between the load line deflections measured by the various laboratory techniques cause less scatter in the J-R curves and $J_{Ic}$ values than attributable to material variability. Further, J-R curves over the first 1.75 mm of crack extension from both bendbars and compacts were shown to be coincident for the alloys tested.



## ADMINISTRATIVE INFORMATION

This report was prepared as a part of the Surface Ship and Craft Materials Block under the sponsorship of Mr. C. Zanis, Naval Sea Systems Command (SEA 05R25). This effort was performed at this Center under Program Element 62761N, Task Area SF 61-541-592, Work Unit 1-2814-210-09.


## INTRODUCTION

Resistance curve characterizations of materials made using three point bend specimens (hereafter bendbars) frequently exhibit more scatter in inter-laboratory data comparisons than do characterizations made using compact tension specimens.[1]* The lack of a convenient location for attachment of a deflectometer on the load line has led to a lack of agreement regarding the proper way to measure load line deflection. Consequently, several different techniques for measuring this quantity have arisen. These fall into two categories; direct methods that measure load line deflection using some

*References are listed on page 43.

transducer, or indirect methods that infer load line deflection from some other displacement quantity measured during testing. These inconsistent measurement techniques have been blamed for the lack of comparability of inter-laboratory bendbar data.

Joyce and Hackett[2] employed a direct method, measuring load line deflection with a thin elastic bar loaded in four point bending by pins protruding from the bendbar. Calibration of this transducer, or "flex bar," prior to each test provided a relationship between displacement at the center of the bar and the output of the strain gage bridge affixed to the bar. Using this calibration and readings from the flex bar taken during the fracture test allowed the determination of load line displacement.

A technique described in the proposed J-R curve testing standard[3] requires that a record of the testing machine cross head displacement be made during fracture testing. Load line deflection is determined by subtracting from these values the cross head displacement attributable to elastic compression and brinelling of the testing machine and test fixtures. The load versus cross head displacement relation thus derived incorporates a component of elastic compliance unique to an individual test setup. Consequently, a new relation must be determined each time any component of the setup is changed.

Because they require taking another channel of data beyond crack mouth opening displacement ($d_{CMOD}$) and load typically required in compact tension tests, both methods discussed heretofore somewhat complicate J-R curve testing of bendbars. Alternatively, a relationship that infers load line displacement from $d_{CMOD}$ could be used. This relationship could be determined using the same assumptions of rigid rotation about a plastic hinge-point used to derive crack tip opening displacement from $d_{CMOD}$[4] or using an experimentally derived correlation. Such a relationship, if justifiable, could considerably simplify data acquisition requirements of bendbar testing.

This investigation focuses on the accuracy of these four methods of approximating the load line deflection during bendbar testing. Photographs taken during testing will provide an absolute reference against which all load line deflection measurements will be compared. Also, blunt notched specimens will be tested to determine the accuracy of the measurements at large deflections in the absence of crack extension. Further, J-R curves from the bendbar tests will be compared to those obtained from compact tension specimens of the same material.

## EXPERIMENTAL PROCEDURE

### MATERIAL AND TEST SPECIMENS

J-R characterizations were developed using specimens from both a 38.1-mm (1.5-in.)-thick 3 Ni steel plate and a 25.4-mm (1-in.) thick ASTM A-710 steel plate. All specimens were notched in the T-L orientation. Table 1 presents both the mechanical properties and the chemical compositions for these materials. Bendbars, compact tension specimens, and an unnotched calibration bar were tested. Figure 1 shows drawings of all specimens with nominal dimensions for each. The Type B bendbars, having the deeper initial notch ($a_o$ = 33 mm) were not precracked prior to testing.

TABLE 1 - CHEMICAL AND MECHANICAL PROPERTY DATA

| | A-710 (GES) | 3-Ni (FYB) |
|---|---|---|
| C | 0.050 | 0.153 |
| Mn | 0.620 | 0.330 |
| P | 0.011 | 0.012 |
| S | 0.004 | 0.013 |
| Cu | 1.050 | 0.033 |
| Si | 0.300 | 0.180 |
| Ni | 0.880 | 2.550 |
| Cr | 0.720 | 1.660 |
| Mo | 0.185 | 0.370 |
| V | - | 0.003 |
| Ti | - | 0.001 |
| $S_{ys}$* | 614 MPa (89 ksi) | 650 MPa (93 ksi) |
| $S_{uts}$* | 731 MPa (106 ksi) | 731 MPa (106 ksi) |
| % Elong.* | 28% | 23% |
| % R. A.* | 74% | 63% |

*All mechanical properties measured using 12.88-mm (0.505-in.) diameter tensile specimens having a gage length of 50.80-mm (2 in.). Specimens were pulled transverse to the plate rolling direction.

## THREE POINT BEND TESTING

Testing was performed in a 266 Newton (60-kip) screw driven testing machine using a modified version of the computer interactive procedure of Joyce and Gudas[5] to control data acquisition. Figure 2, a schematic of the test setup, indicates that four channels of data were recorded. A clip gage attached slightly above the specimen's front face was used to determine $d_{CMOD}$ while load and cross head displacement came from the load cell and the LVDT on the testing machine respectively. Figure 3 shows a detail of the flex bar and how it is attached to the bend specimen. It is calibrated prior to testing by applying a known displacement at its center and observing the resulting signal from the strain gage bridge. This calibration allows determination of load line deflection during the fracture toughness test. Photographs of the specimen were taken on Kodak Plus-X film using a Nikon FE camera with a 50-mm Nikkor macro lens. Each photo was taken as the test came out of an unloading so that the crack length would be known. The Type B bendbars were not unloaded during the test because the presence of the blunt notch prevented significant crack extension. These specimens were photographed at roughly equivalent intervals of load or load line deflection. Subsequent to testing, the specimens were heat tinted to mark the final extent of crack growth and broken open at liquid nitrogen temperatures.

## COMPACT TENSION TESTING

Compact tension tests were performed on both materials using the computer interactive procedure of Joyce and Gudas.[6] This procedure follows the guidelines set forth in ASTM testing standard E-813.

# LOAD LINE DEFLECTION MEASUREMENTS

## MEASURED FROM PHOTOGRAPHS

Bendbars were photographed during testing. Load line deflection measured from enlargements of the photographs using a digitizing tablet served as a reference against which all other measures of load line deflection were compared. To determine the load line deflection the distance between the loading tup and the horizontal reference bar was measured. This distance was then reduced by the distance between the loading tup and the horizontal reference bar before loading began measured off the reference photograph. Figure 4 illustrates this procedure.

Two factors limit the accuracy of photographic load line deflection measurements; the resolution of the digitizing tablet and motion of the horizontal reference bar. The tablet was accurate to +/- 0.0635 mm (+/- 0.0025 in.) and the magnification of the photographs was 2X, thus making the overall accuracy +/- 0.0318 mm (+/- 0.00125 in.), assuming consistent placement of the digitizing cross hair. To minimize error resulting from inconsistent cross hair placement each point was digitized multiple times and the average of the repeated measurements was calculated. Repeated mesaurement was terminated when oscillation of the average value subsided to less than 0.0508 mm (0.002 in.).

Because the horizontal reference bar is mounted on pins protuding from the specimen, specimen deformation also limits the accuracy of the photographic load line deflection measurements. Assuming that the specimen rotates as two rigid halves, as shown in Figure 5, allows estimation of influence of this downward motion. This assumption leads to the following relation between percent error in the photographic measurement and the amount of load line deflection.

$$\text{percent error} = h_o\{1 - \text{COS}\,[\,\text{SIN}^{-1}(2D_{LL}/S)]\} * 100/D_{LL} \qquad (1)$$

where

$h_o$ = original height of reference bar support point from specimen front face, 33.375 mm (1.313 in.)

$S$ = span between rollers, 203.2 mm (8 in.)

$D_{LL}$ = load line deflection

Figure 6 shows the effect of both sources of error as a function of load line displacement. Generally the error is small, less than three percent, except at load line deflections less than 1 mm (0.039 in.) where the error due to limited digitizing pad resolution becomes quite large. For this reason, load line deflections measured from the photographs of less than 1 mm were excluded from subsequent analysis.

MEASURED FROM FLEX BAR TRANSDUCER

Load line deflection from the flex bar was determined during testing using the linear calibration established prior to each test. No further data manipulation is necessary.

CALCULATED FROM CROSS HEAD DISPLACEMENT

To determine the load line deflection from measurements of cross head displacement the displacement attributable to machine compliance must be subtracted. This was determined using the procedure outlined in the proposed J-R curve testing standard.[3] A solid bar of A-710 having the same overall dimensions as the test specimens was loaded to 125% of the maximum load encountered during any of the testing. Load and cross head displacement were recorded and the cross head displacement was reduced by that attributable to the bar, given by Euler beam theory as

$$D_{BAR} = PS^3/48EI \qquad (2)$$

where

P = load applied at mid span

S = span between roller supports

E = Young's modulus

I = moment of inertia

to determine the cross head displacement due only to machine compliance. Figure 7 shows these results graphically.

CALCULATED FROM CLIP GAGE MEASUREMENTS

Load line deflection may be determined from $d_{CMOD}$ by assuming that the bend-bar rotates as two rigid halves about a plastic hinge. Referring to Figure 5, the following relation holds if the angle of specimen rotation remains small:

$$D_{LL}{}^{d} = Sd_{CMOD}/2(W-\beta b) \qquad (3)$$

where

S = span between roller supports

W = specimen width

$\beta$ = an empirical coefficient expressing fraction of b around which the remaining ligament is assumed to hinge

b = uncracked ligament

At larger deflections, where this assumption becomes invalid, then

$$D_{LL}^{drc} = [S/2 - Wd_{CMOD}/2(W-\beta b)] \text{ TAN } \{\text{SIN}^{-1} [d_{CMOD}/2(W-\beta b)]\} \quad (4)$$

A value of $\beta = 0.6$ was used, as suggested by Garwood.[6] Figure 8 gives these equations in graphical form. The effects of specimen rotation are not significant until $d_{CMOD}$ exceeds 0.254 mm (0.010 in).

An alternative to a relationship between $D_{LL}$ and $d_{CMOD}$ based on rigid rotation assumptions would be to experimentally determine the relation between these two displacements. Figure 9 shows load line deflection measured from the photographs as a function of $d_{CMOD}$ for all specimens tested. The slope of this line is relatively insensitive to material, sidegrooving, amount of specimen rotation, and degree of plastic deformation prior to crack initiation. Consequently, a linear relationship shows promise for determining load line deflection from $d_{CMOD}$ data. In order to use these data to predict $D_{LL}$ from $d_{CMOD}$ a zero intercept line of the form

$$D_{LL}^{corr} = md_{CMOD} \quad (5)$$

was fit to the data in Figure 9 using the method of least squares. To avoid a biased prediction, the data from a given specimen was not used to determine the m coefficient (slope) used on that specimen's $d_{CMOD}$ data. Table 2 gives the slope values used for the specimens tested.

TABLE 2 - EMPIRICAL CORRELATION SLOPES RELATING LOAD LINE DISPLACEMENT TO CRACK MOUTH OPENING DISPLACEMENT

| Specimens Deleted | m (slope) |
|---|---|
| GES-40 | 1.1630 |
| FYB-511 | 1.1584 |
| FYB-512 | 1.1624 |
| GES-44 | 1.1609 |
| GES-45 | 1.1459 |
| FYB-503 | 1.1694 |

## RESULTS AND DISCUSSION

Load versus load line deflection curves, with displacement measured using all of the methods discussed above, are shown in Figures 10 and 11 for an A-710 and a 3-Ni steel specimen respectively. Data from each displacement measurement technique is shown with the data from the photographic reference. In both cases the specimen deviating most from the photographic reference is shown.

To facilitate easier comparison of the load line deflection measured from the photographs to displacement measurements from each technique these data were plotted against each other. Figure 12 shows the comparison plots; an intercept of zero and a slope of one indicates perfect agreement with the photographic reference. Least squares analysis given in Table 3 shows that the best fit values for the various methods do not deviate very far from this ideal. In each case the fit slope and intercept showed minor dependencies on material and crack extension. As these were small and of relatively constant magnitude in each comparison, subsequent analysis treated all data in Figure 12 as one group and did not distinguish between different specimens.

TABLE 3 - LEAST SQUARES COEFFICIENTS FOR COMPARISONS OF DEFLECTION MEASUREMENTS TO PHOTOGRAPHIC REFERENCE

| Measurement Technique | Intercept | Slope |
|---|---|---|
| Flex Bar | -0.0032 | 1.0549 |
| Cross Head | -0.0025 | 0.9956 |
| $D_{LL}^{d}$ | 0.0004 | 1.0559 |
| $D_{LL}^{drc}$ | 0.0020 | 1.0237 |
| $D_{LL}^{corr}$ | 0.0023 | 0.9824 |

Because of the error in the photographic measurements shown in Figure 6 it is not appropriate to rank the various load line deflection measurements with respect to their ability to match the ideal slope and intercept values. Rather, if the data in Figure 12 falls within a region about the ideal line determined by the error bounds in Figure 6 it cannot be said to deviate significantly from the photographic reference values. Figure 13 shows this acceptable data region. To determine how well the data from each technique falls within this region the residual, or vertical distance of each point from the acceptable data region, was calculated for each point. Points lying within the acceptable data region had no residual. The average residual for each measurement technique was then calculated as follows:

$$\text{RESIDUAL} = \sum_{r=1}^{n} (r_i^2)/n \qquad (6)$$

where

$r_i$ = residual of the $i^{th}$ data point, vertical distance from the acceptable data region shown in Figure 13

n = total number of data points

Table 4 gives the average residual values for each measurement technique tried; all are small with the largest being 0.052 mm (0.0020 in). Because the average residuals are so close for every technique, varying only 0.009 mm (0.0004 in) from lowest to highest, it must be concluded that all techniques match the photographic data equally well over the range of load line deflections observed in this investigation.

TABLE 4 - AVERAGE RESIDUALS OF EACH MEASUREMENT TECHNIQUE FROM THE PHOTOGRAPHIC REFERENCE

| Measurement Technique | Residual mm (in) |
|---|---|
| Flex Bar | 0.052 (0.0020) |
| Cross Head | 0.042 (0.0016) |
| $D_{LL}^{d}$ | 0.047 (0.0019) |
| $D_{LL}^{drc}$ | 0.046 (0.0018) |
| $D_{LL}^{corr}$ | 0.043 (0.0017) |

Because the result of a fracture toughness test is either a J-R curve or a $J_{IC}$ value it is important to show how these small differences in load line deflection measurements among the various techniques translate into differences in fracture property characterizations. To this end, both J-R curves and $J_{IC}$ values were calculated using the formulae and procedures described in ASTM Standard Test Method E-813 and the tentative J-R curve test procedure[3] for the three bendbars that experienced crack extension. Figure 14 shows the J-R curves overlayed with 95% confidence bands from two specimens of the same material. As the data scatter from the various load line deflection measurement techniques is less than the material scatter, shown by the 95% bands, differences in J-R curves due to the different techniques can be considered insignificant. Table 5 gives $J_{IC}$ values for these same tests. Comparing the ranges of $J_{IC}$ for the different load line deflection measurements to the ranges given for each material leads to the same conclusion as made for the J-R curve data. That is that small differences among the various load line deflection measurements tried remain small when the data is used to calculate a $J_{IC}$ value.

TABLE 5 - $J_{Ic}$ VALUES

| Specimen | Measurement Technique | $J_{Ic}$ kPa*m (in*lb/in$^2$) |
|---|---|---|
| GES-40 (A-710) | Flex Bar | 188 (1075) |
| | Cross Head | 184 (1050) |
| | $D_{LL}{}^{d}{}_{drc}$ | 204 (1164) |
| | $D_{LL}{}_{corr}$ | 202 (1155) |
| | $D_{LL}$ | 193 (1104) |
| FYB-511 (3-Ni) | Flex Bar | 148 (846) |
| | $D_{LL}{}^{d}{}_{drc}$ | 155 (888) |
| | $D_{LL}{}_{corr}$ | 154 (881) |
| | $D_{LL}$ | 146 (836) |
| FYB-512 (3-Ni) | Flex Bar | 137 (780) |
| | $D_{LL}{}^{d}{}_{drc}$ | 144 (822) |
| | $D_{LL}{}_{corr}$ | 143 (816) |
| | $D_{LL}$ | 135 (768) |

A-710 Material Scatter Range: 188 to 234 kPa*m (1075 to 1335 in*lb/in$^2$)
3-Ni Material Scatter Range: 137 to 148 kPa*m (780 to 846 in*lb/in$^2$)

A disparity has at times been noted between the fracture mechanics values determined using bendbar and compact tension specimens. Figure 15 shows the J-R characterizations for the three bendbars that experienced crack extension overlayed with data from two compact tension specimens of the same alloy. Good agreement between the J-R data from the two geometries exists over the accpetable data range given in the tentative J-R curve test procedure[3] which limits the maximum crack extension to 10% of the initial remaining ligament, or approximately 1.75 mm (0.070 in). At longer crack extensions larger deviations between the J values from the two geometries occur. While this may be attributed to uncertanties in bendbar load line deflection measurements, uncertainties in the J-integral formulation or differences in constraint between the two geometries may also play a role.

## SUMMARY

The following conclusions may be drawn from this work:

1. Statistical comparisons of load line deflection measurements to the photographic reference data shows that all techniques match the photographic data equally well (within 0.052 mm) over the range of load line deflections observed (0 mm to 8 mm) in this investigation;
2. The small differences among the various load line deflection measurement techniques investigated cause small differences in J-R curves and $J_{1c}$ values that are within the magnitude of scatter due to material variability;
3. Bendbar and compact J-R curve characterizations are coincident over the first 1.75 mm, or 10% of the initial remaining ligament, of crack extension for the alloys tested. At longer crack extensions differences in J determined by the two geometries may be due to uncertainties in bendbar load line deflection, uncertainties in the J formulation, or constraint differences between bendbars and compact tension specimens.

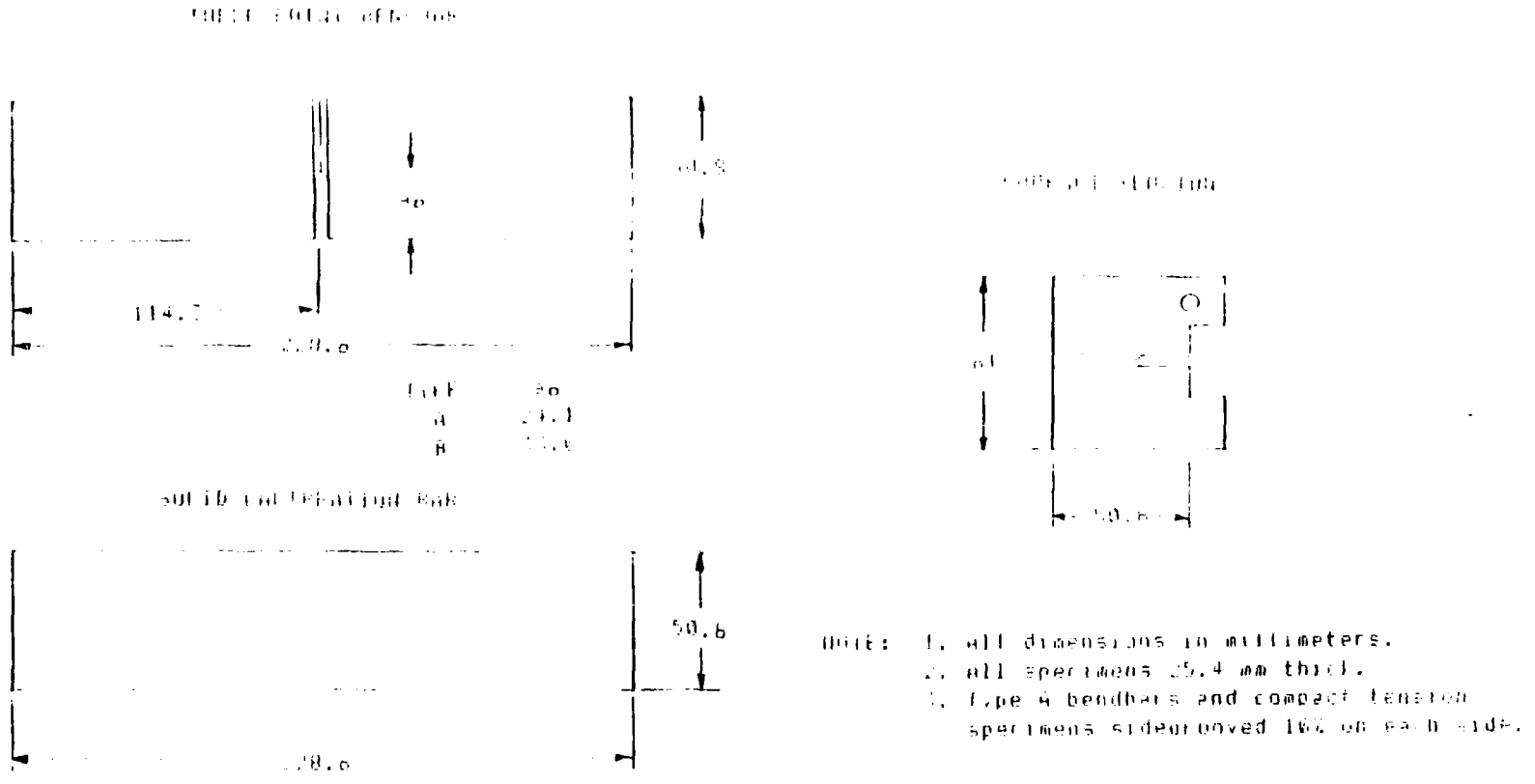


Figure 1 - Diagrams of Specimens Tested

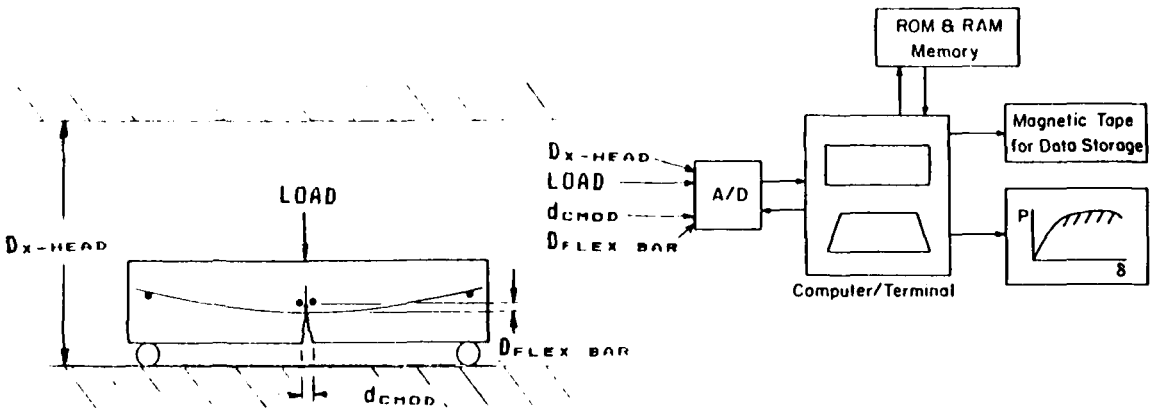


Figure 2 - Schematic of Computer Interactive Test Apparatus

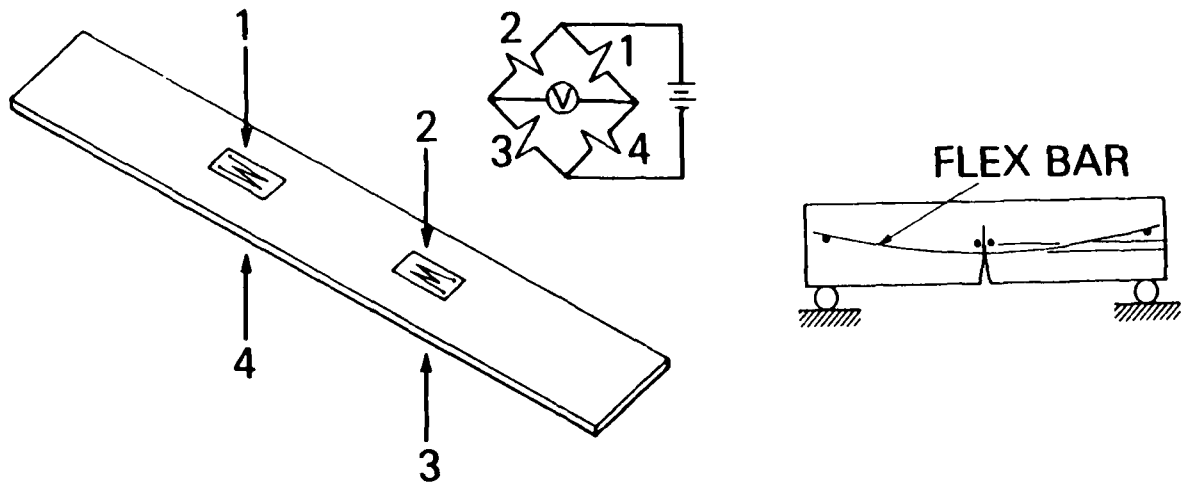


Figure 3 – Schematic of Flex Bar and Its Attachment to Three Point Bend Specimen

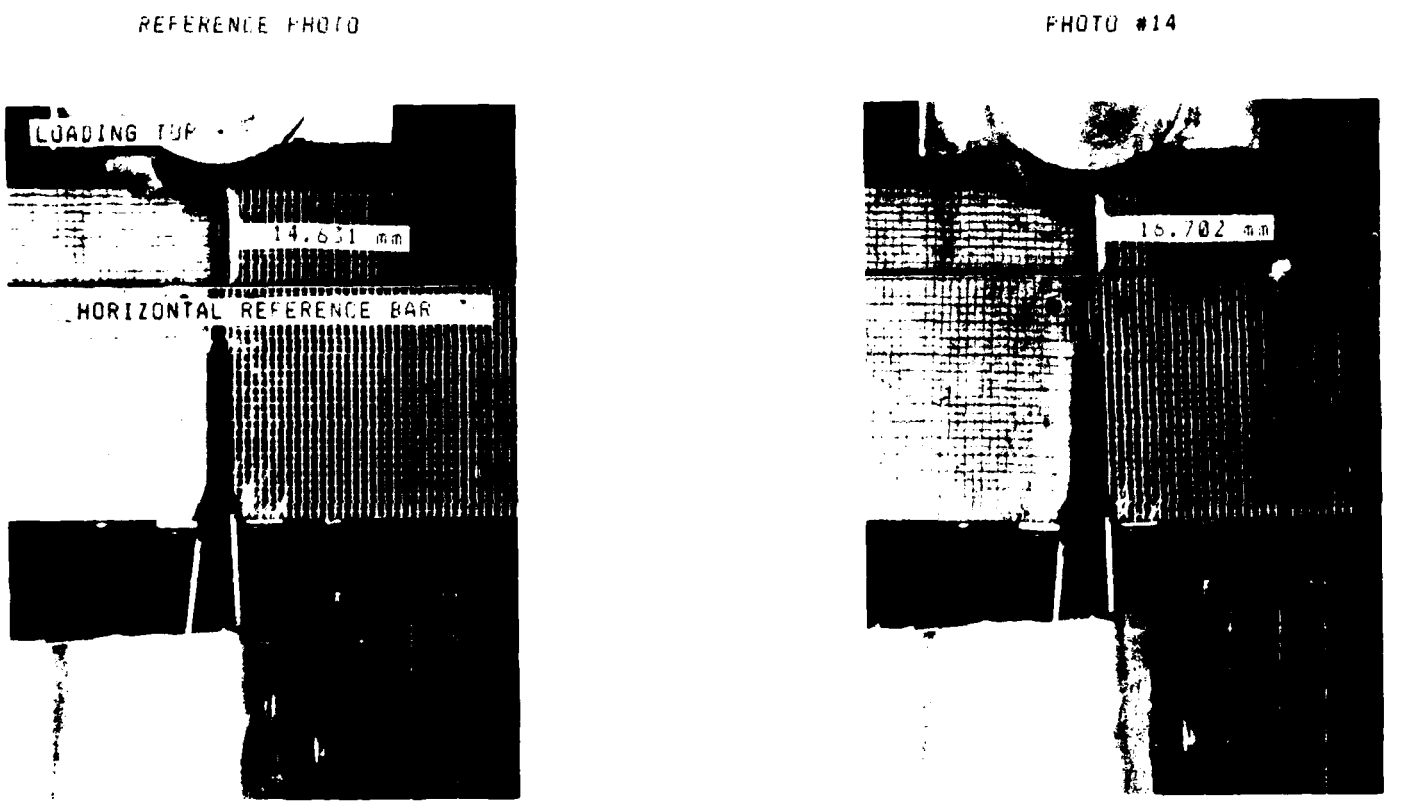


$D_{LL}^{14}$ = 16.702 mm - 14.631 mm = 2.071 mm

Figure 4 - Procedure for Determination of Load Line Displacement from Photographs

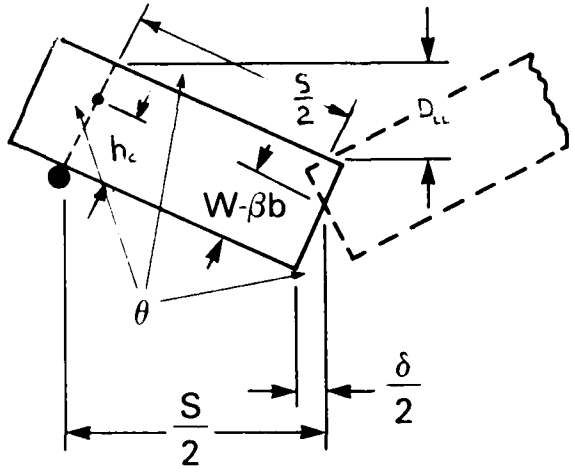


Figure 5 - Diagram Showing Terms Used in Equations Based on Rigid Rotation Assumptions

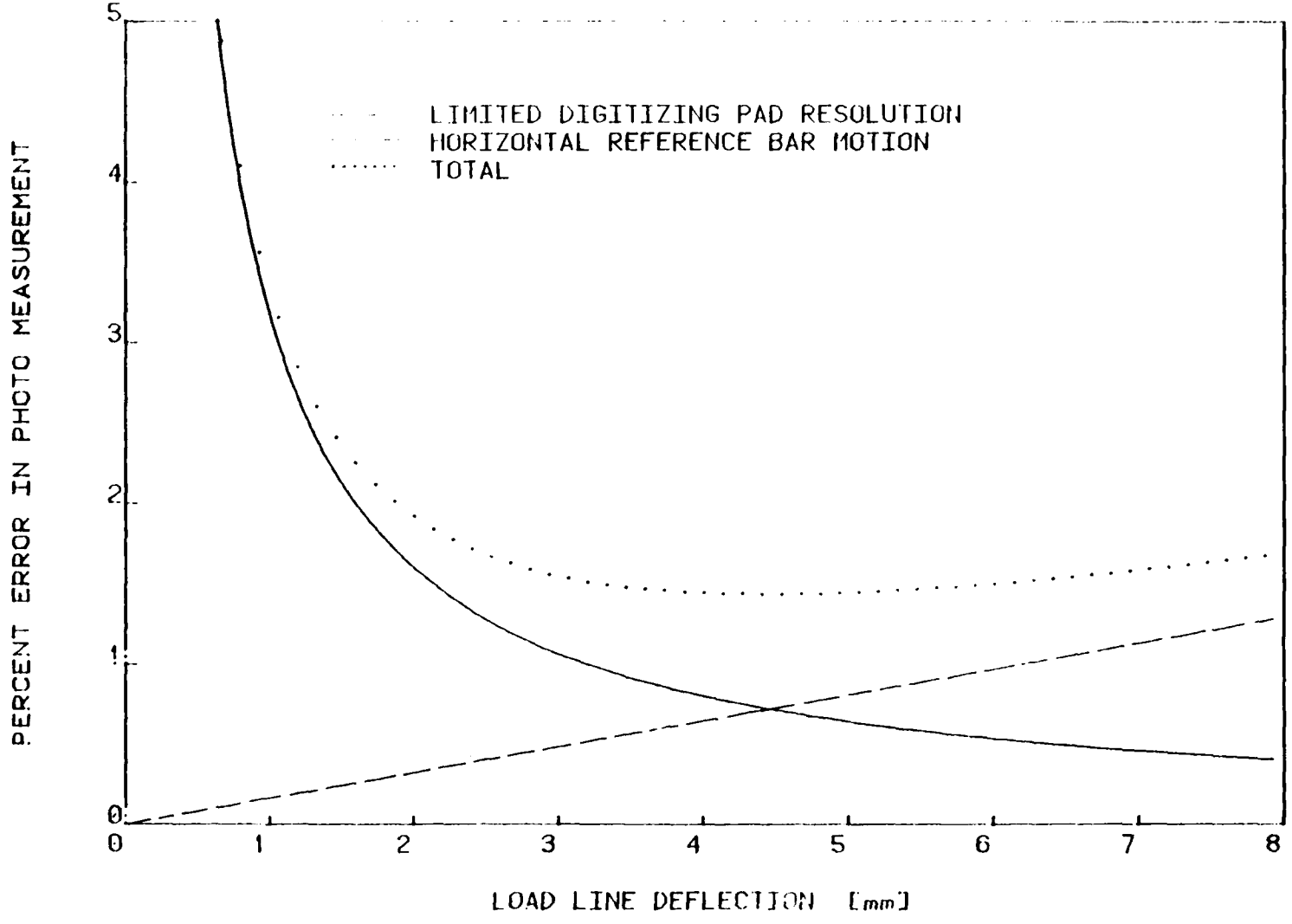


Figure 6 – Expected Error In Load Line Displacement Measurements from the Photographs Due to Limited Digitizing Pad Resolution and Horizontal Reference Bar Motion

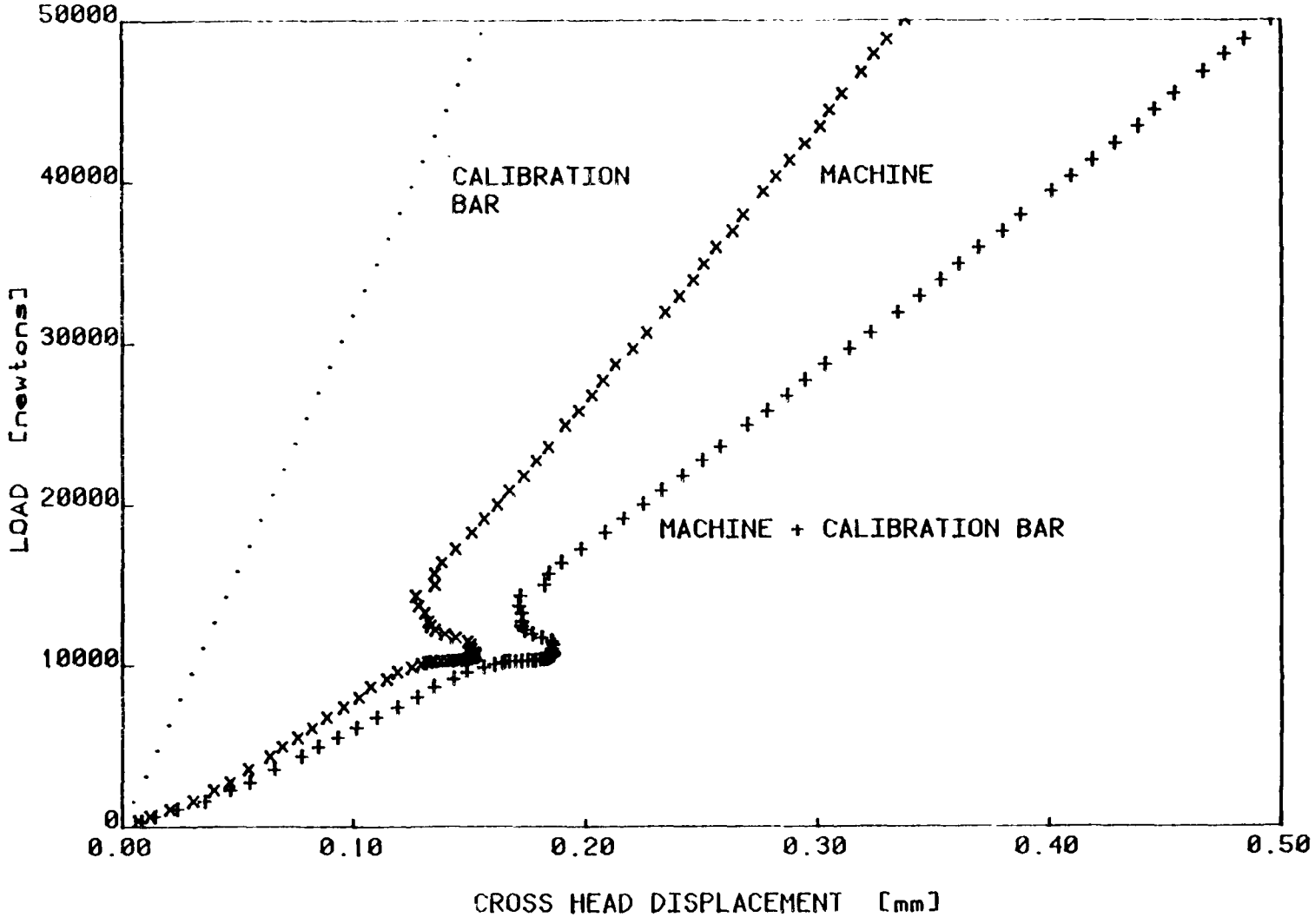


Figure 7 - Load Versus Testing Machine Cross Head Displacement Characteristic

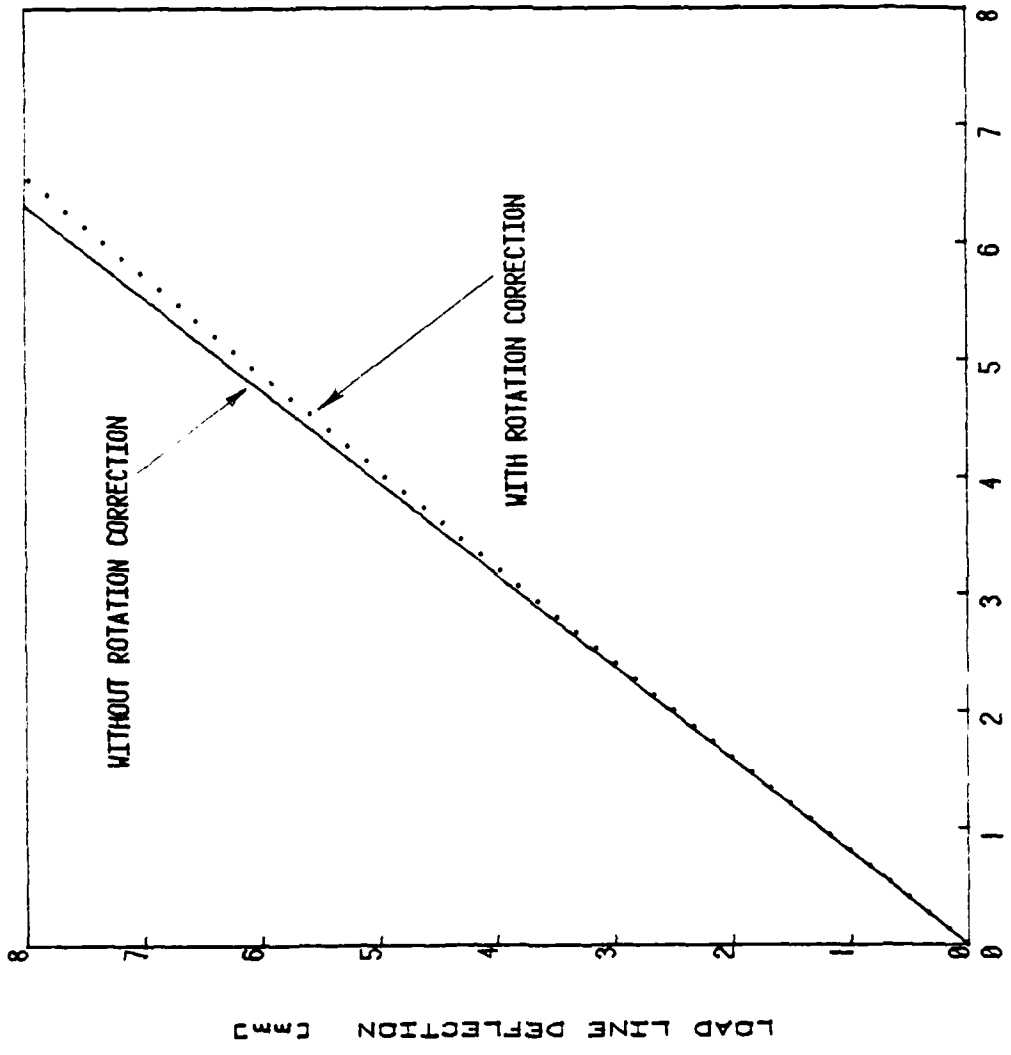


Figure 8 - Relation Between Load Line Deflection and $d_{CMOD}$ Determined Using Rigid Rotation Assumptions

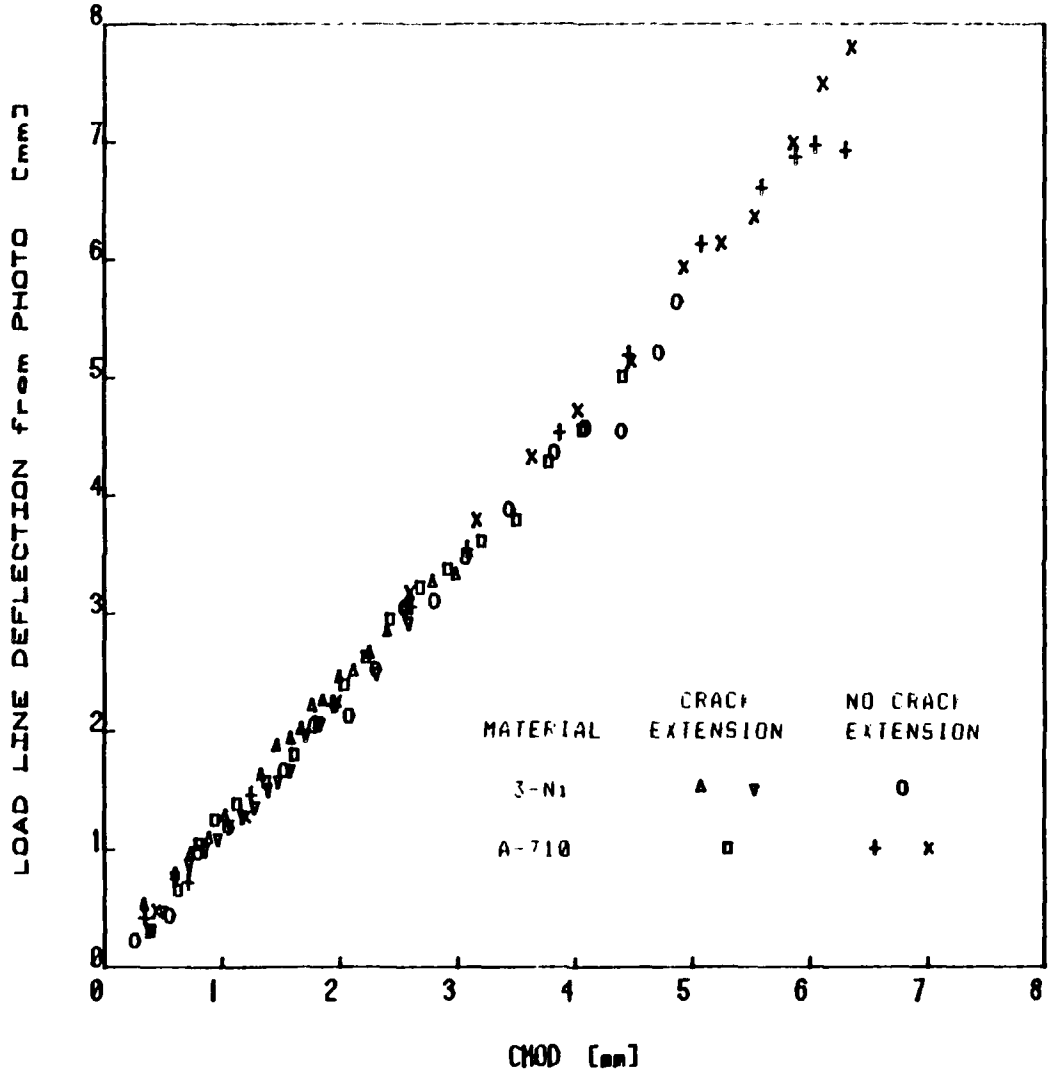


Figure 9 - Relation Between Load Line Deflection and $d_{CMOD}$ Determined Using Empirical Correlation

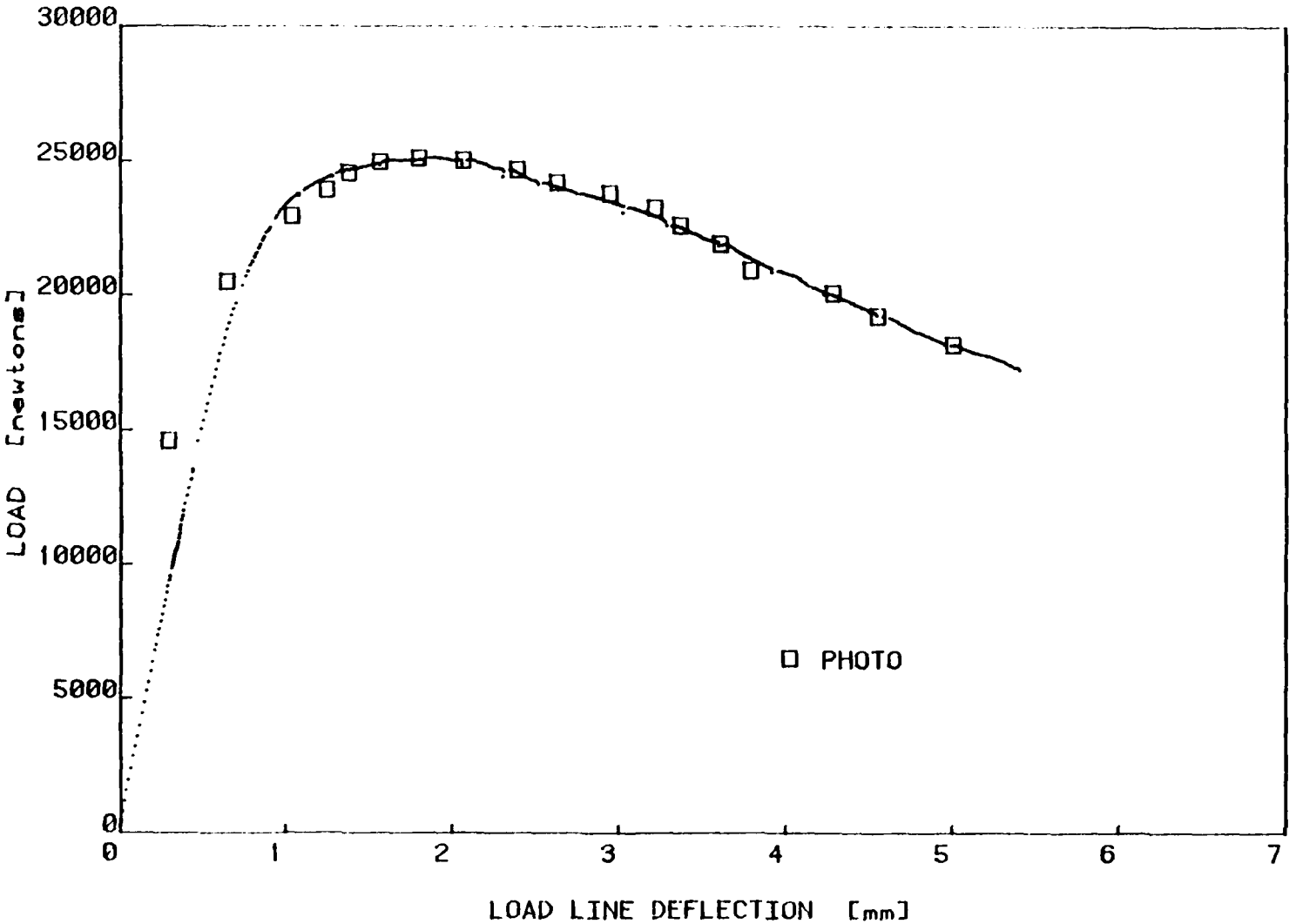


Figure 10a - Load Versus Load Line Deflection Determined Using the Flex Bar Compared to the Photographic Data (A-710 Specimen GES-40)

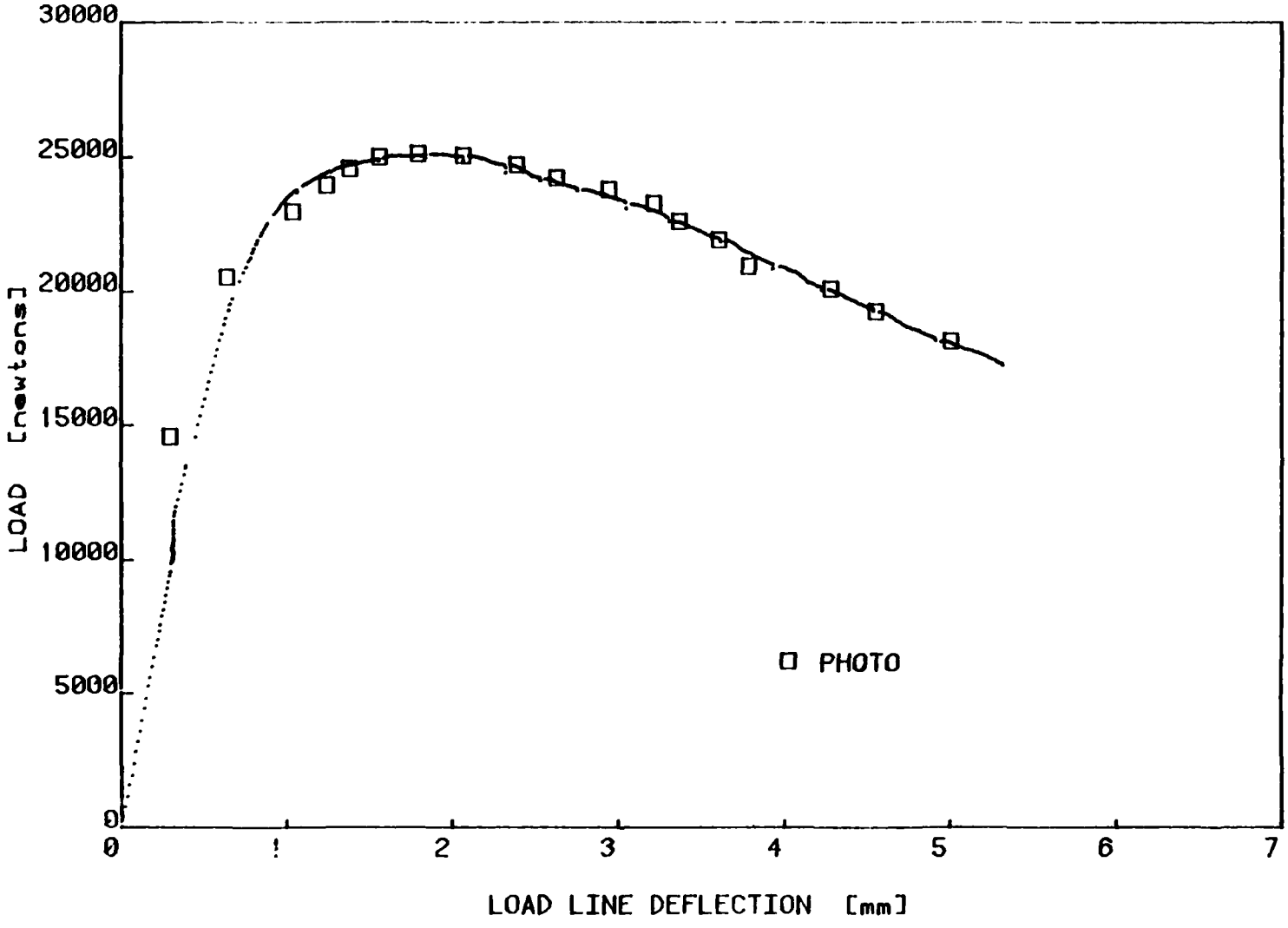


Figure 10b - Load Versus Load Line Deflection Determined Using Cross Head Displacement Corrected for Machine Compliance Compared to the Photographic Data (A-710 Specimen GES-40)

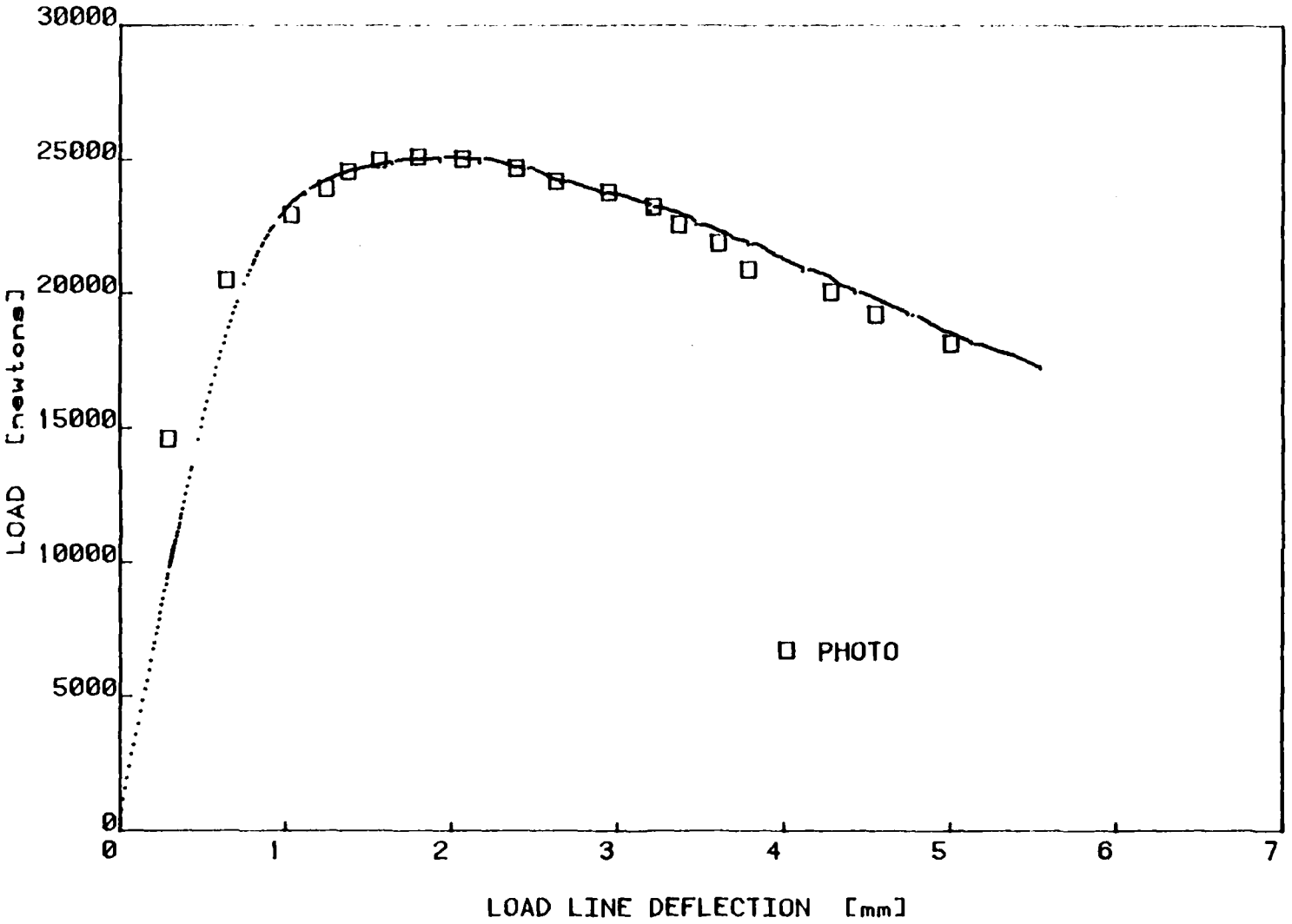


Figure 10c - Load Versus Load Line Deflection Determined Using $d_{CMOD}$ and a Rigid Rotation Assumption Compared to the Photographic Data (A-710 Specimen CES-40)

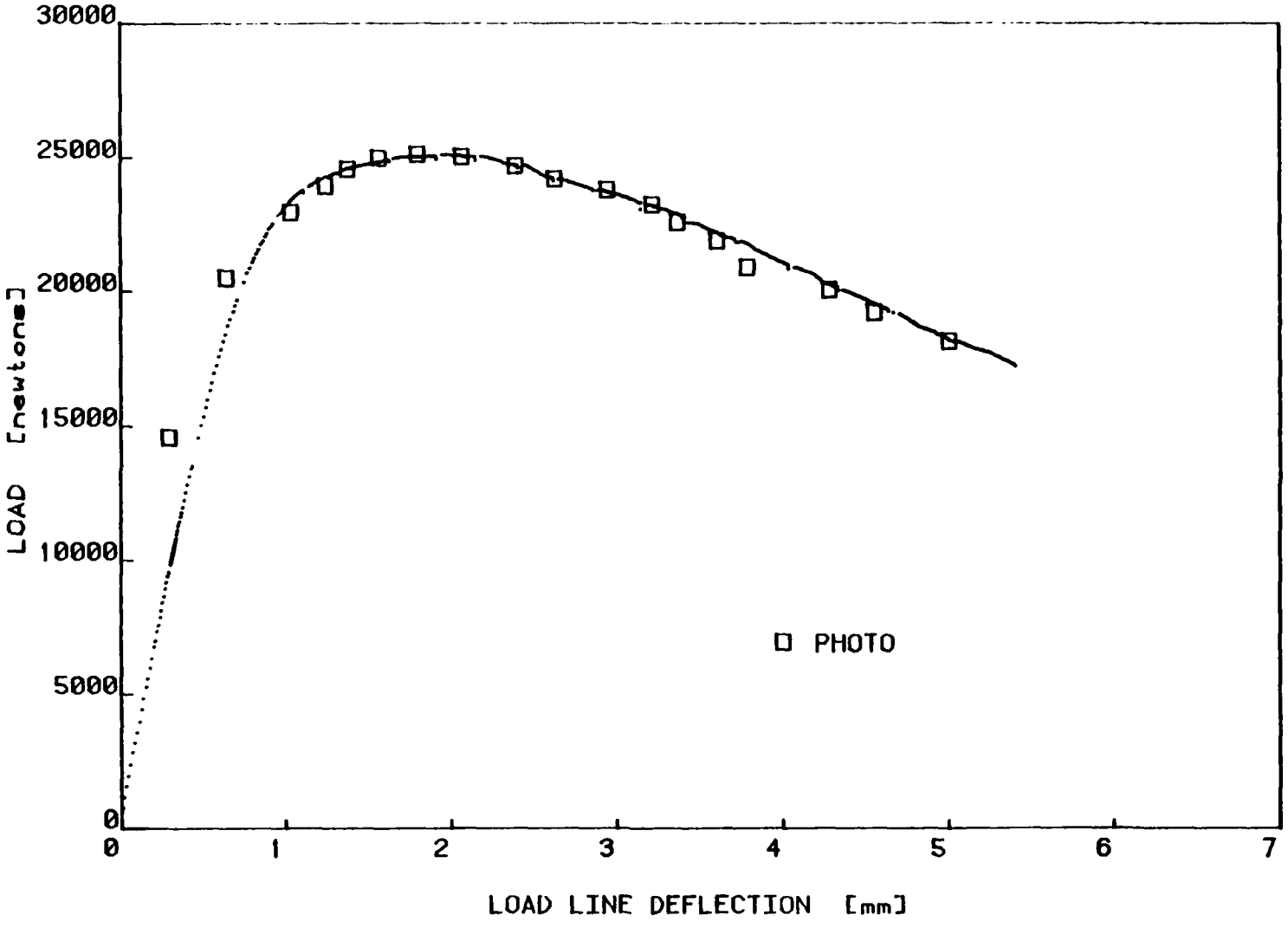


Figure 10d - Load Versus Load Line Deflection Determined Using $d_{CMOD}$ and a Rigid Rotation Assumption Corrected for Specimen Rotation Compared to the Photographic Data (A-710 Specimen GES-40)

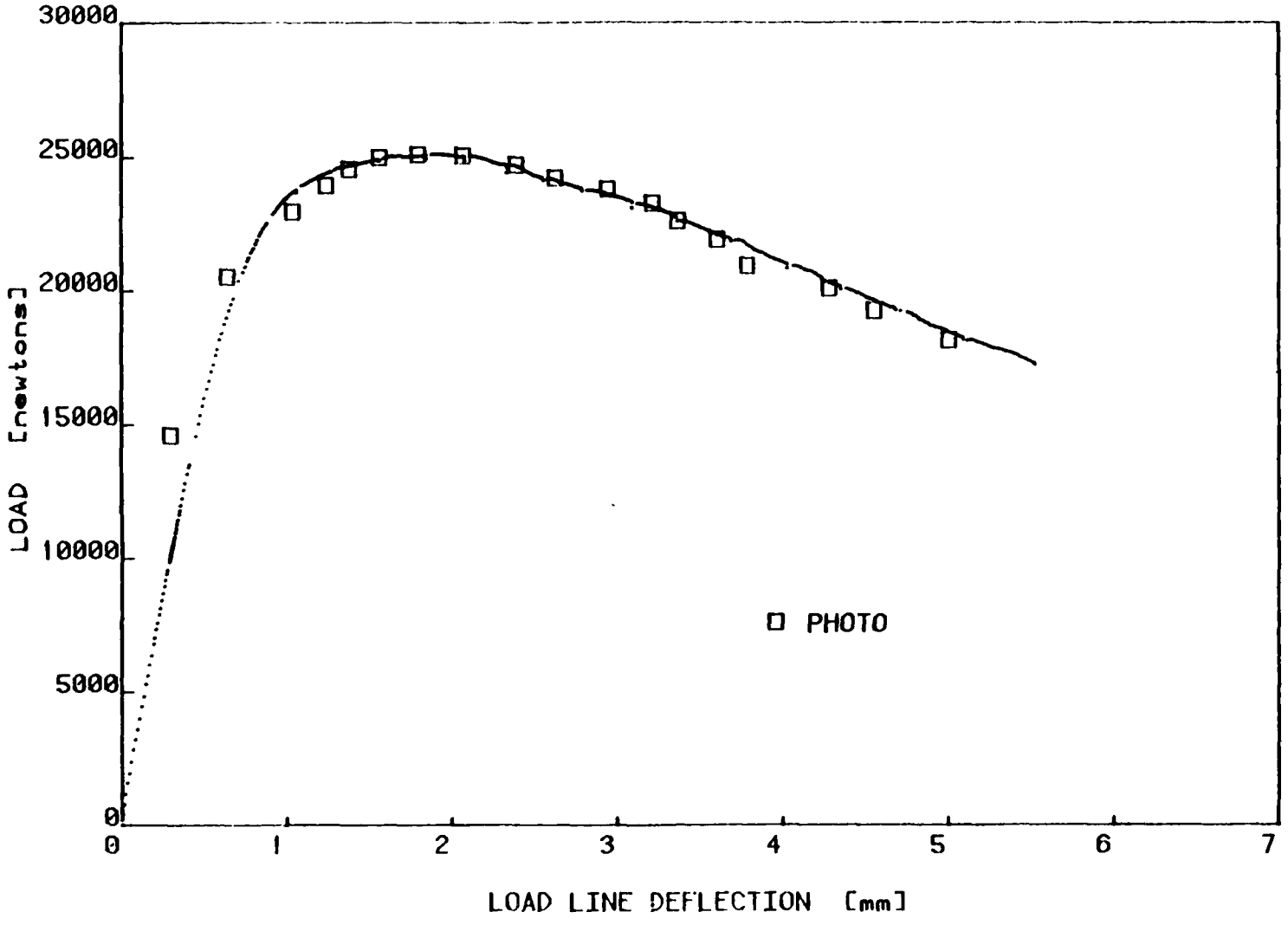


Figure 10e - Load Versus Load Line Deflection Determined Using an Experimentally Derived Correlation Compared to the Photographic Data (A-710 Specimen CES-40)

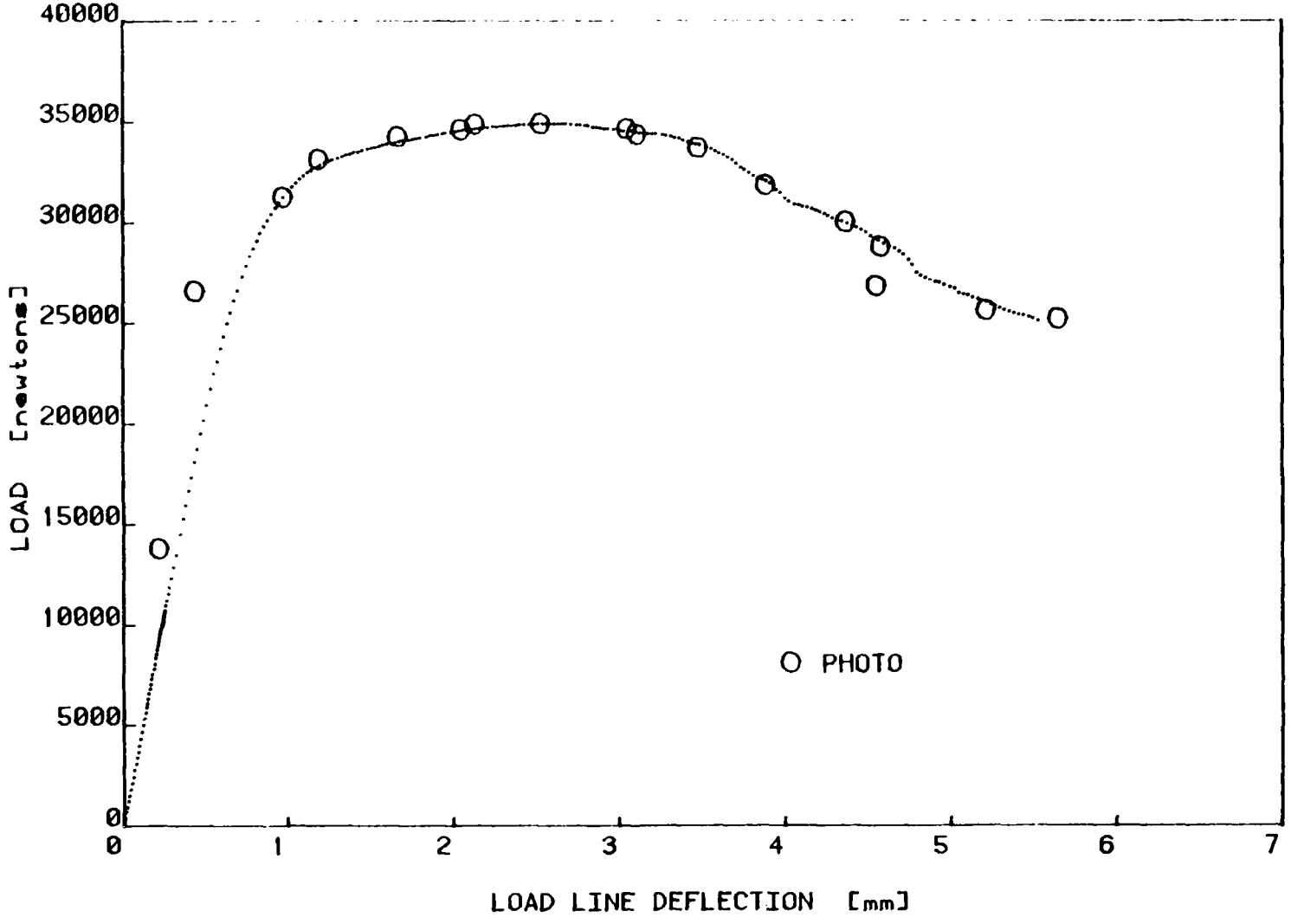


Figure 11a - Load Versus Load Line Deflection Determined Using the Flex Bar Compared to the Photographic Data (3-Ni Specimen FYB-503)

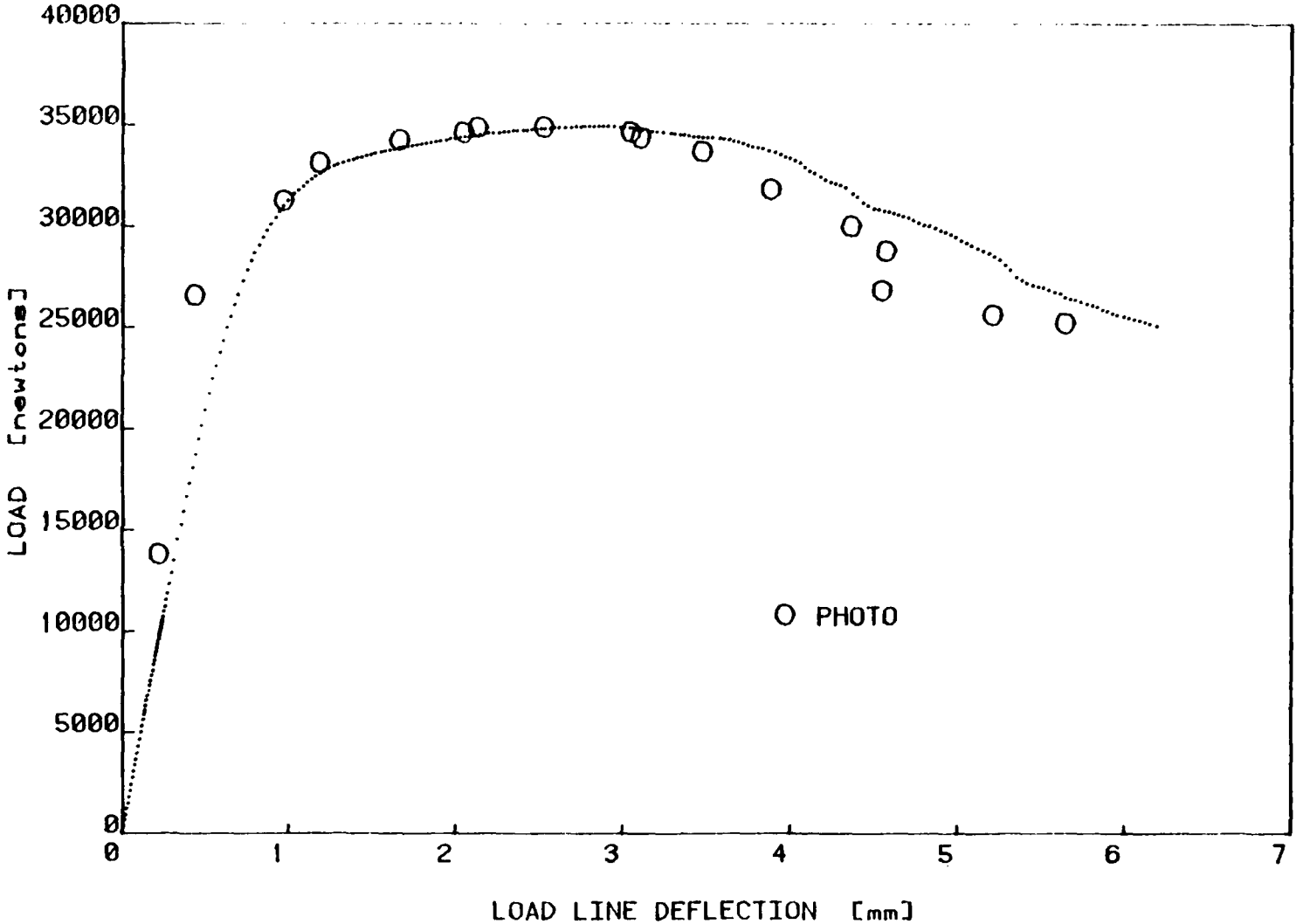


Figure 11b - Load Versus Load Line Deflection Determined Using $d_{CMOD}$ and a Rigid Rotation Assumption Compared to the Photographic Data (3-NI Specimen FYB-503)

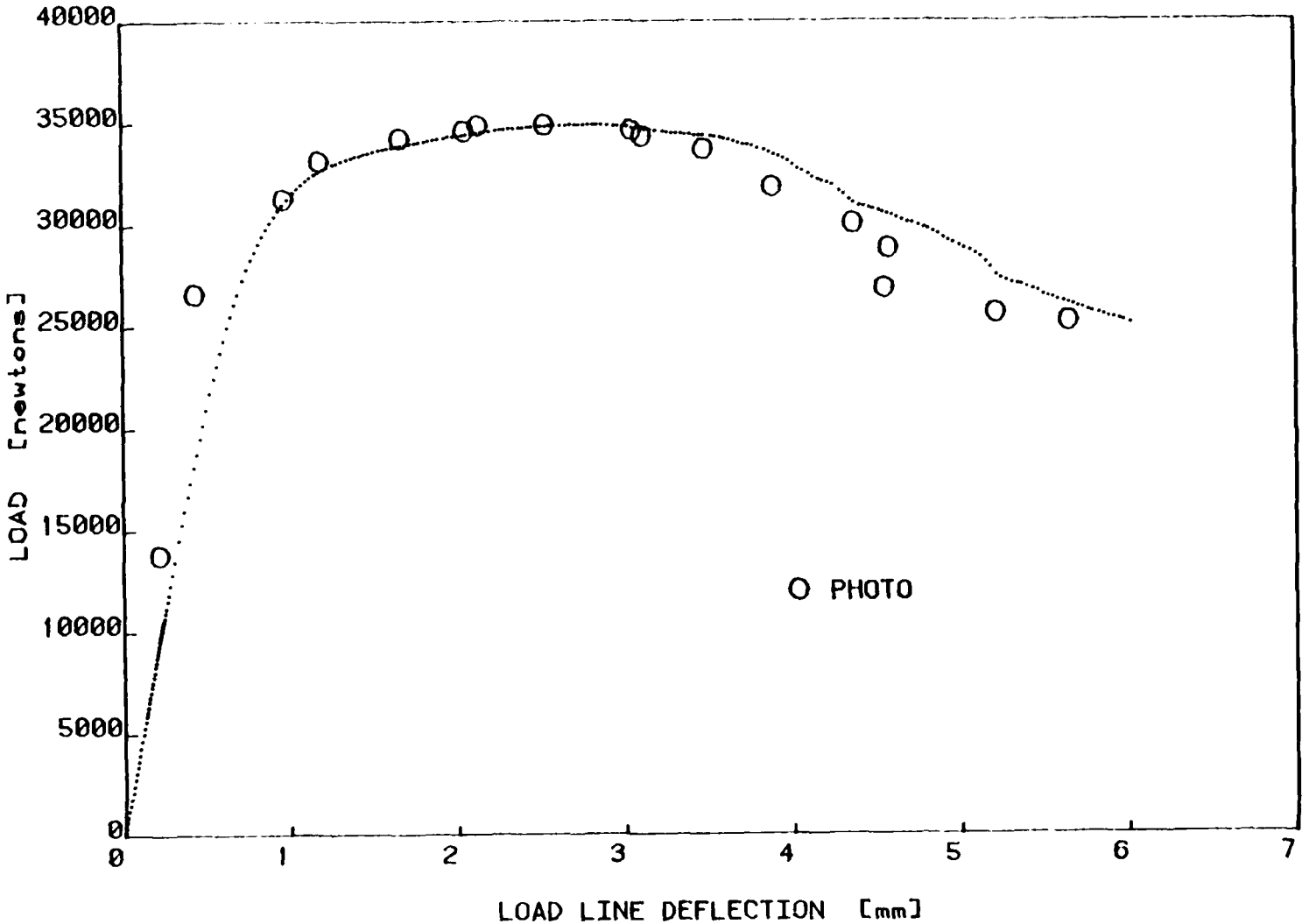


Figure 11c - Load Versus Load Line Deflection Determined Using $d_{CMOD}$ and a Rigid Rotation Assumption Corrected for Specimen Rotation Compared to the Photographic Data (3-Ni Specimen FYB-503)

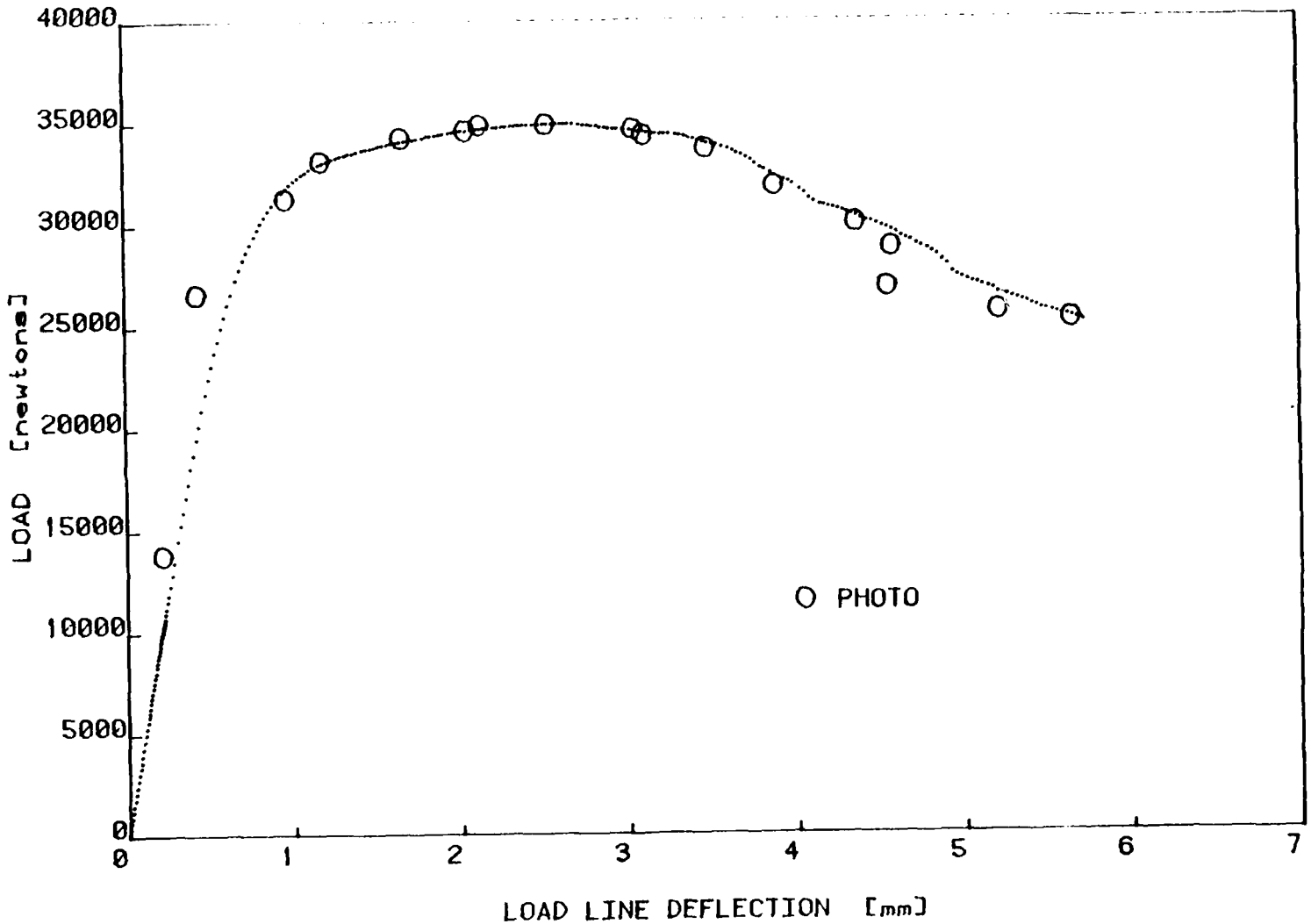


Figure 11d - Load Versus Load Line Deflection Determined Using an Experimentally Derived Correlation Compared to the Photographic Data (3-NI Specimen FYB-503)

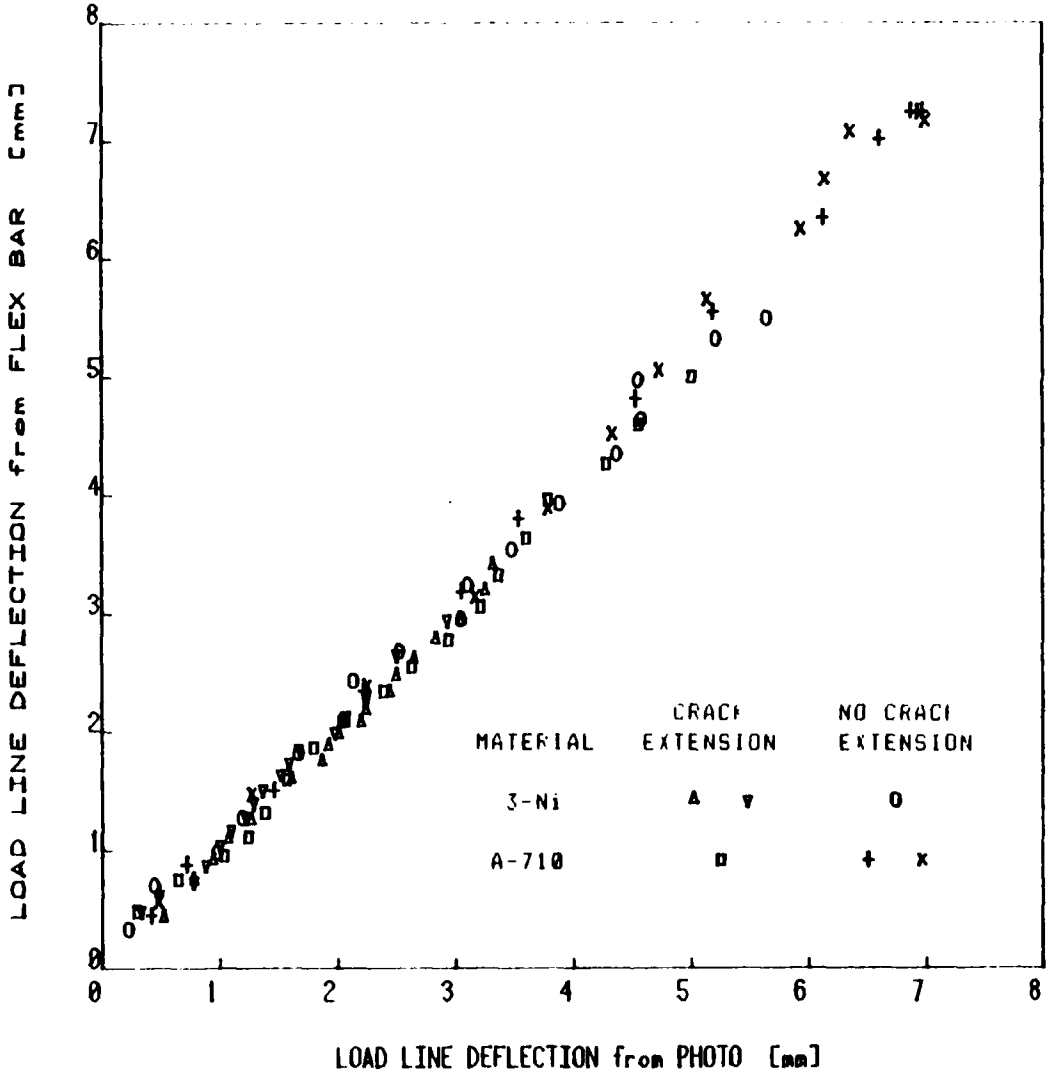


Figure 12a - Comparison of Load Line Deflection Measured Using the Flex Bar to the Photographic Load Line Deflection Measurements

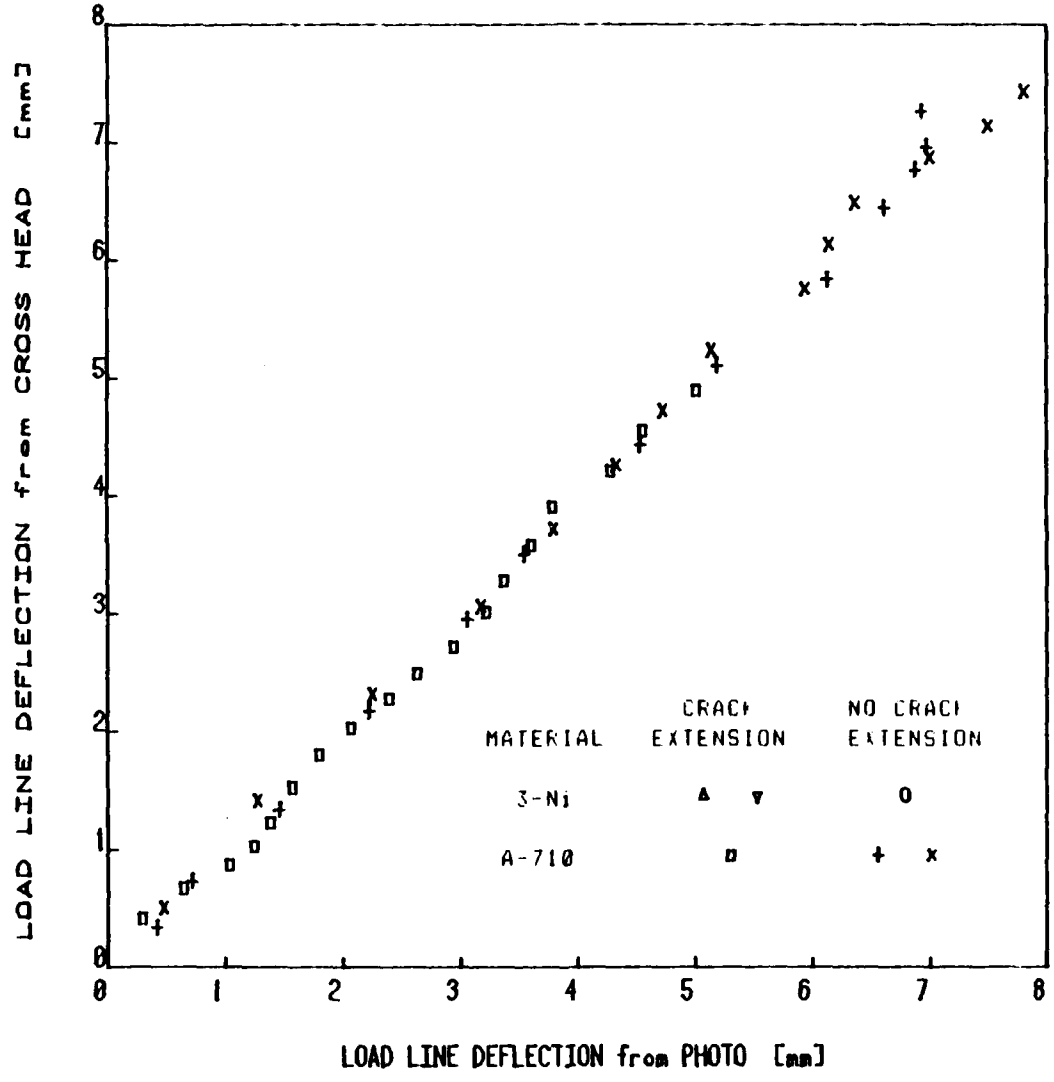


Figure 12b - Comparison of Load Line Deflection Measured Using Cross Head Displacement Corrected for Machine Compliance to the Photographic Load Line Deflection Measurments

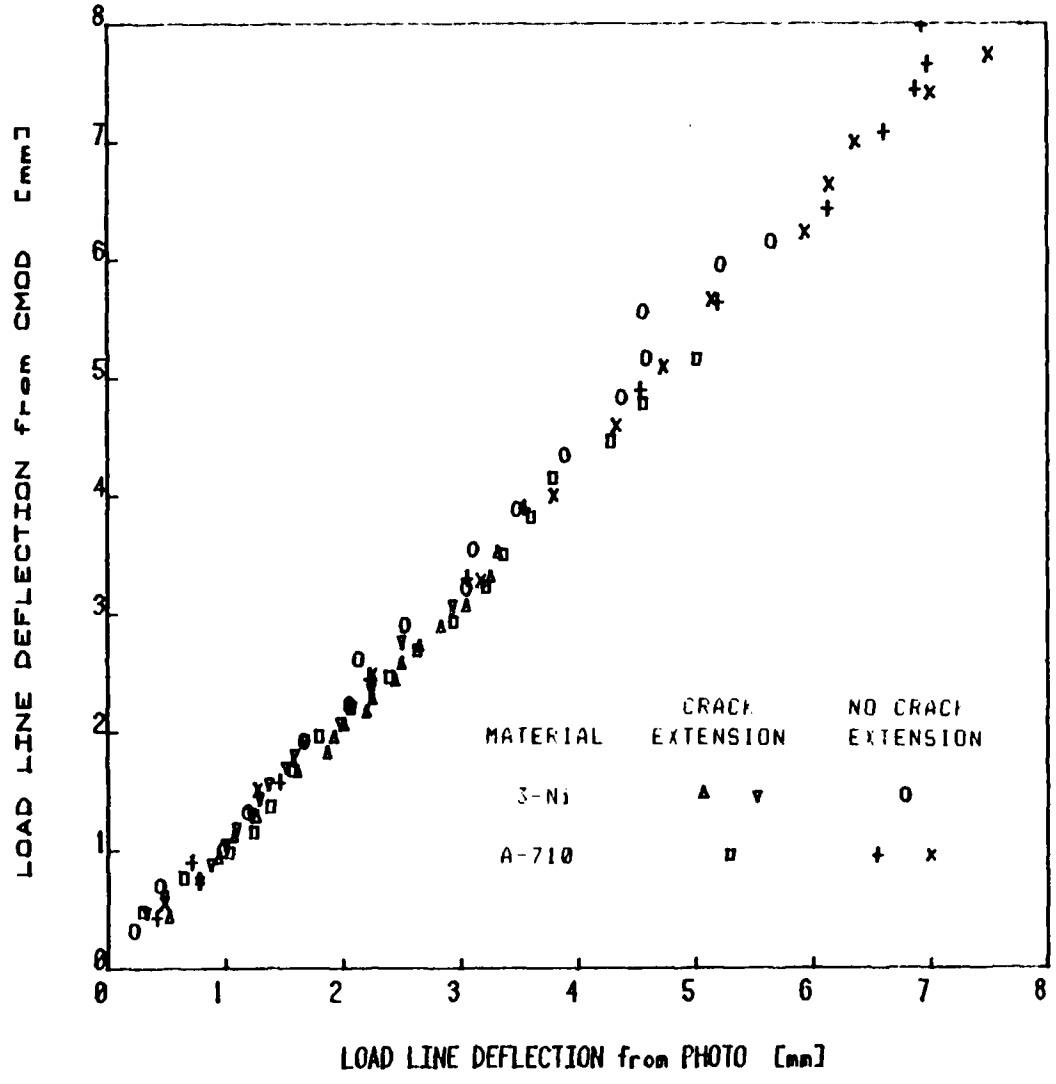


Figure 12c - Comparison of Load Line Deflection Measured Using $d_{CMOD}$ and a Rigid Rotation Assumption the Photographic Load Line Deflection Measurements

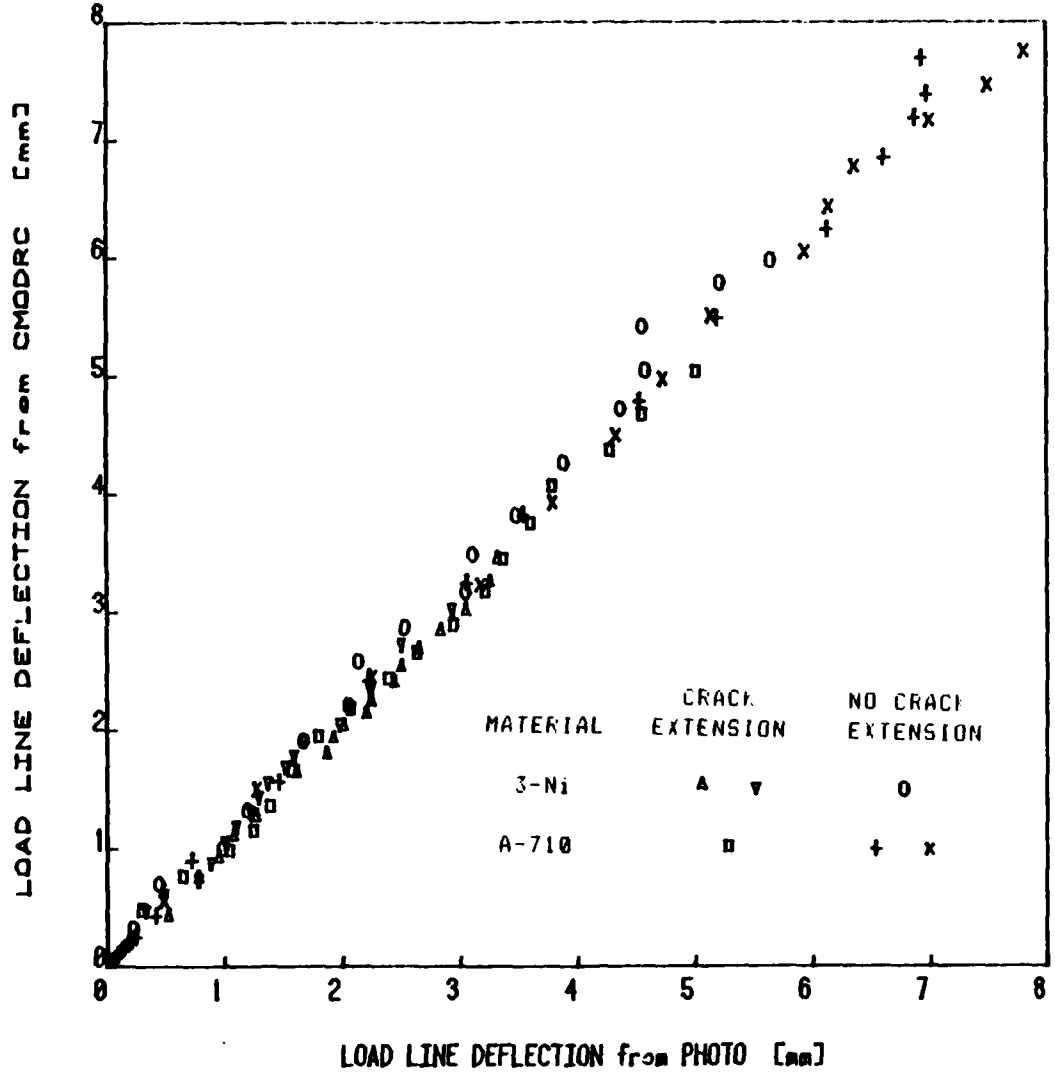


Figure 12d - Comparison of Load Line Deflection Measured Using $d_{CMOD}$ and a Rigid Rotation Assumption Corrected for Specimen Rotation to the Photographic Load Line Deflection Measurments

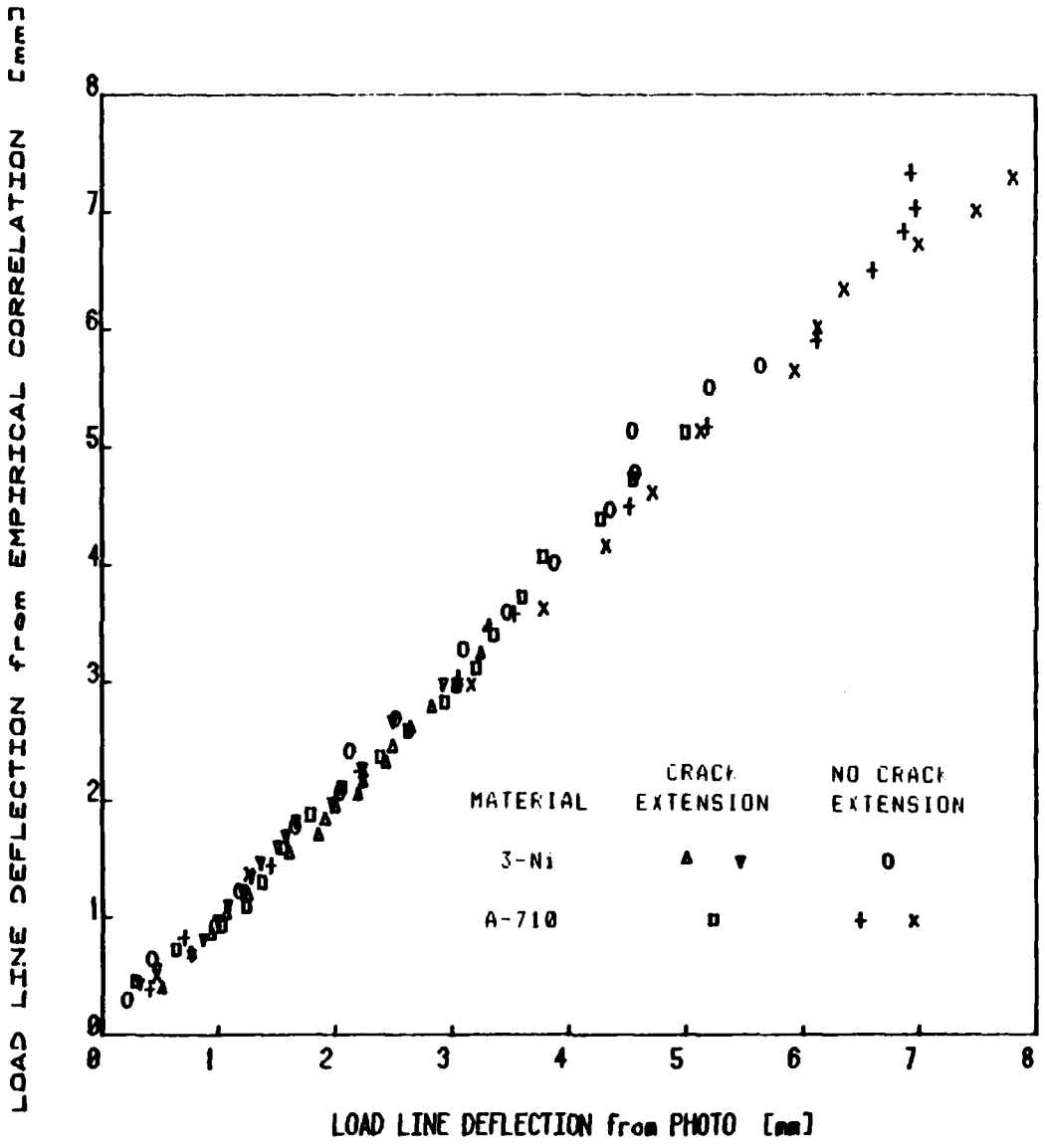


Figure 12e - Comparison of Load Line Deflection Measured Using an Experimentally Derived Correlation to the Photographic Load Line Deflection Measurements

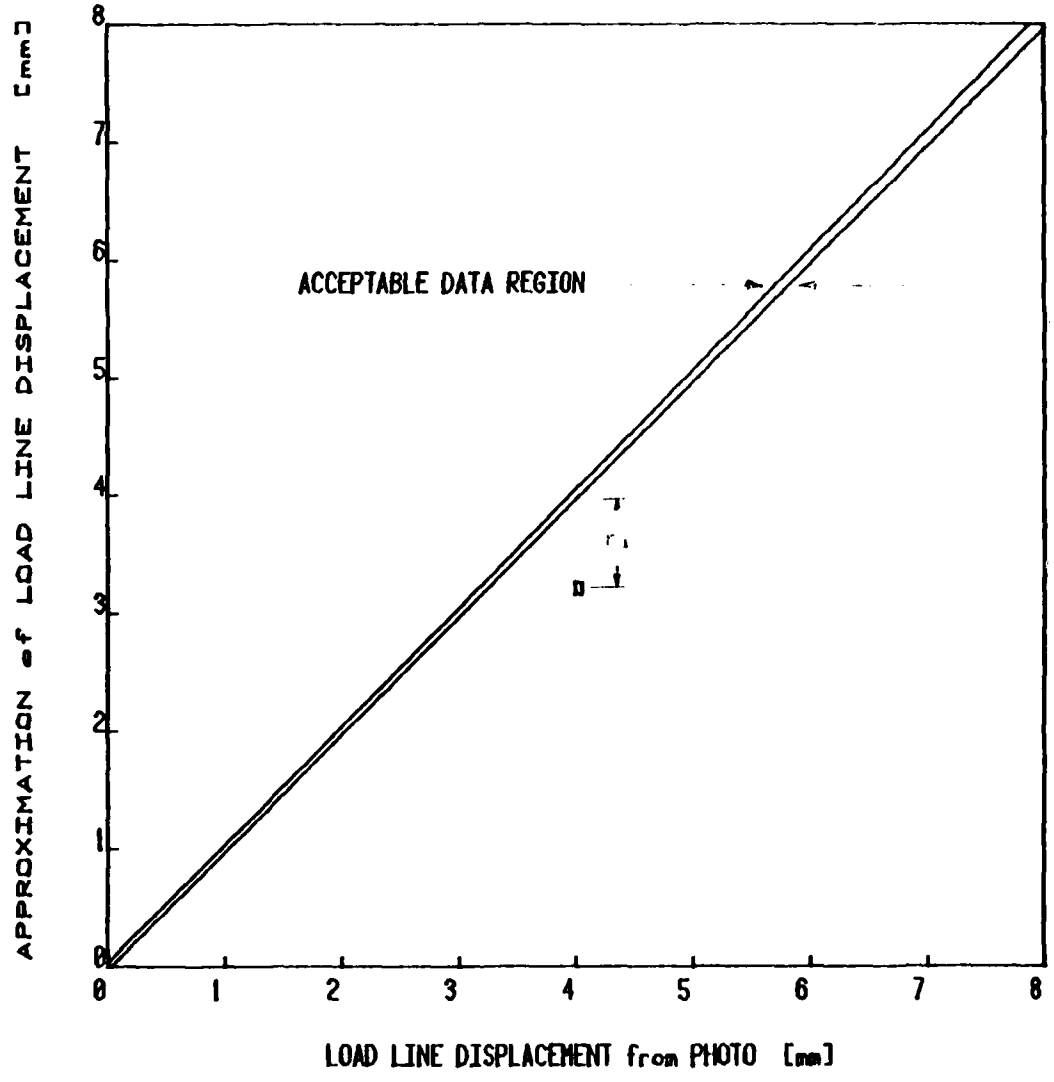


Figure 13 - Plot Showing the Acceptable Data Region and the Residual of a Data Point Lying Outside of the Region

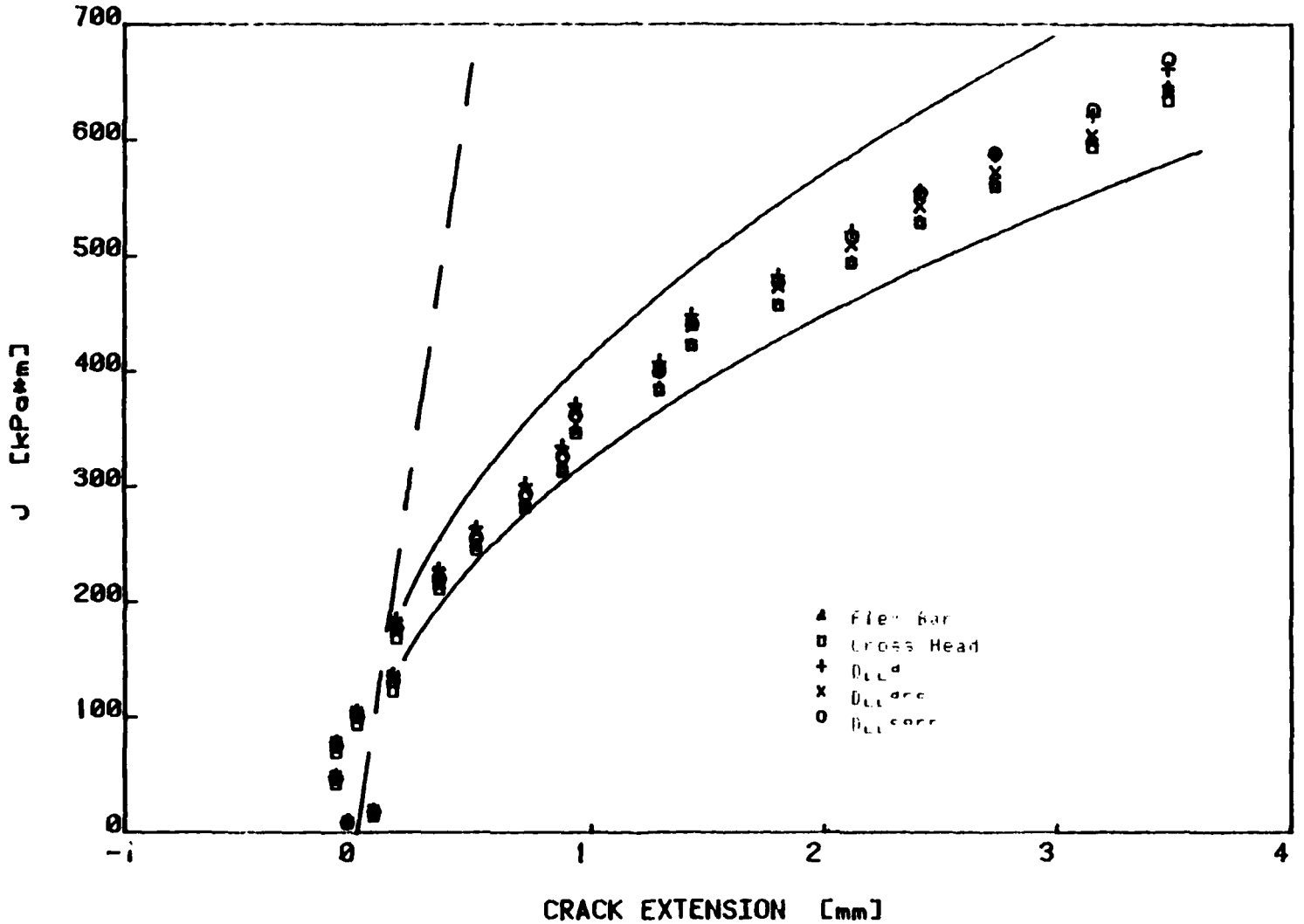


Figure 14a - J-R Curves for A-710 Bendbar GES-40 Showing the Effect of Different Load Line Deflection Measurements (Points) and Material Scatter (95% Confidence Bands)

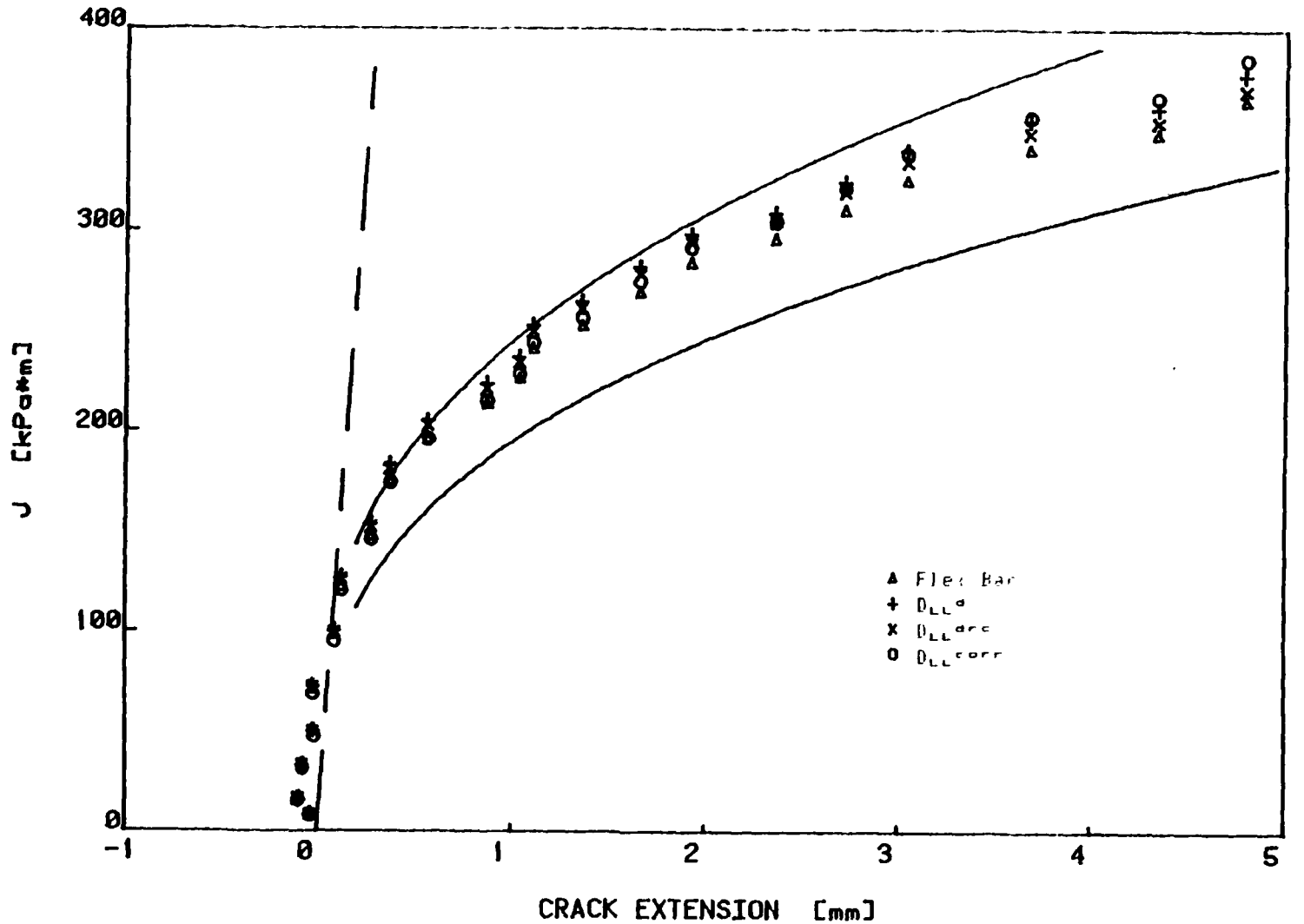


Figure 14b - J-R Curves for 3-Ni Bendbar FYB-511 Showing the Effect of Different Load Line Deflection Measurements (Points) and Material Scatter (95% Confidence Bands)

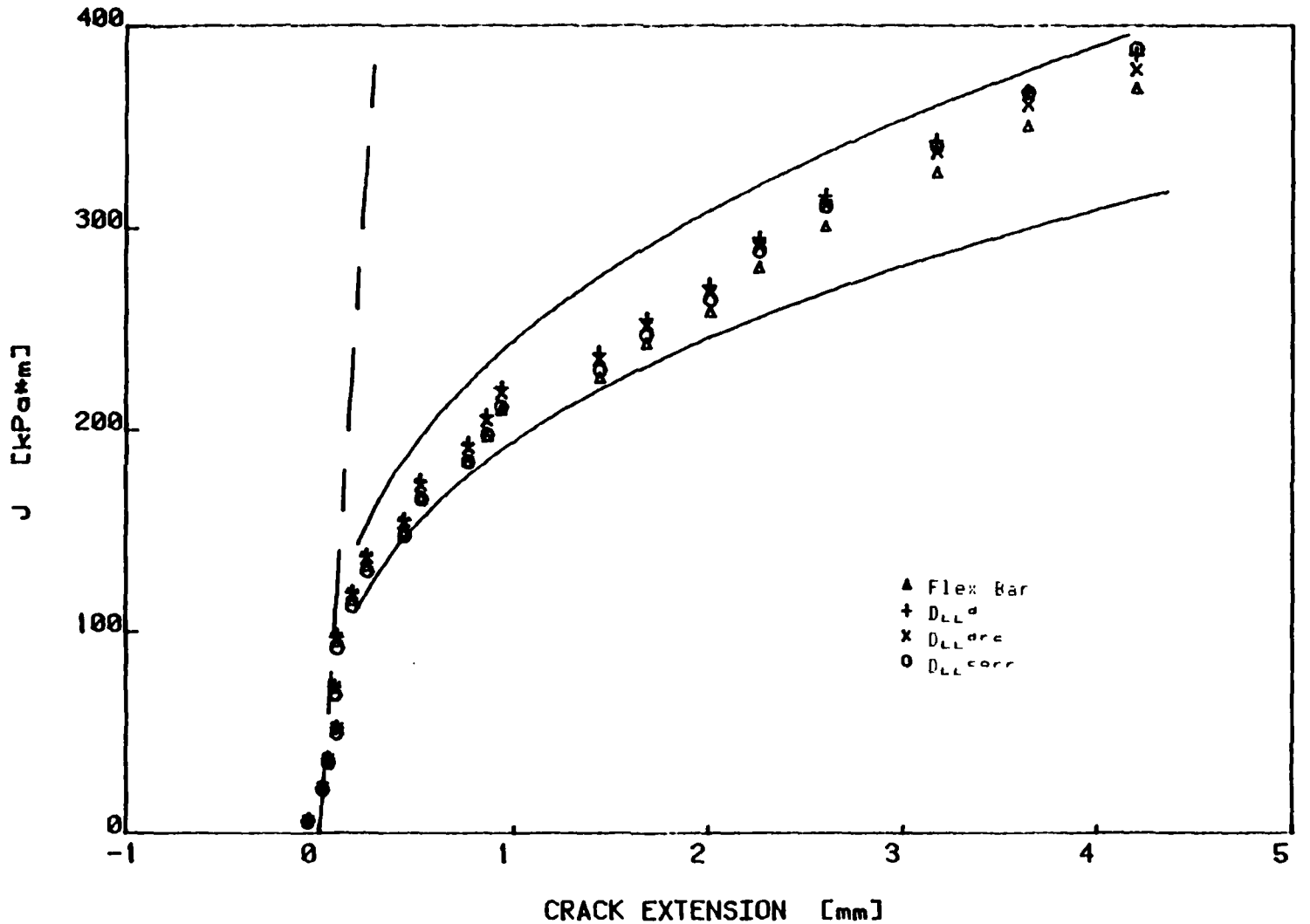


Figure 14c - J-R Curves for 3-Ni Bendbar FYB-512 Showing the Effect of Different Load Line Deflection Measurements (Points) and Material Scatter (95% Confidence Bands)

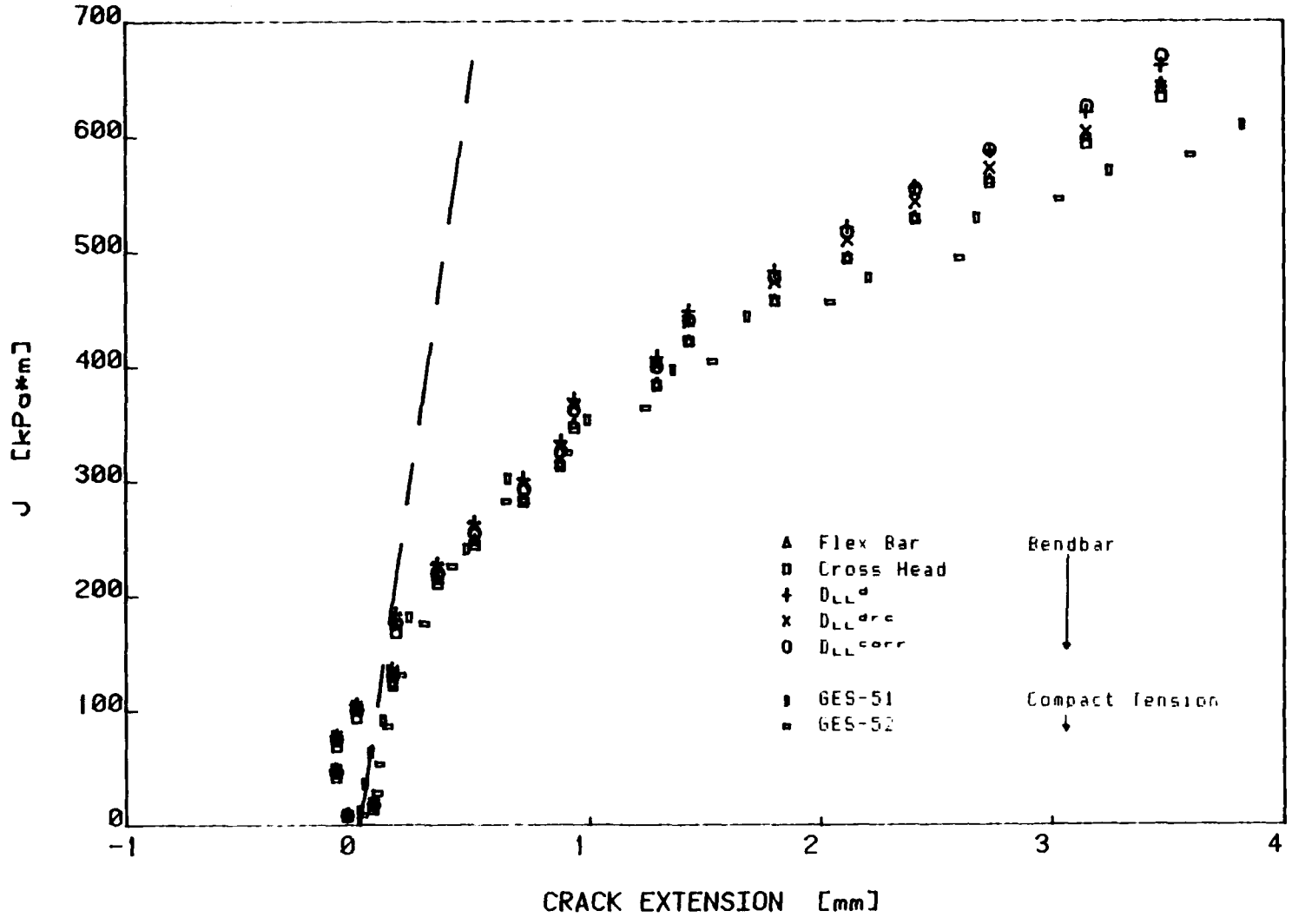


Figure 15a - J-R Curves for A-710 Bendbar GES-40 with Different Load Line Deflection Measurements Compared to Data from Two Compact Tension Specimens of A-710 Steel

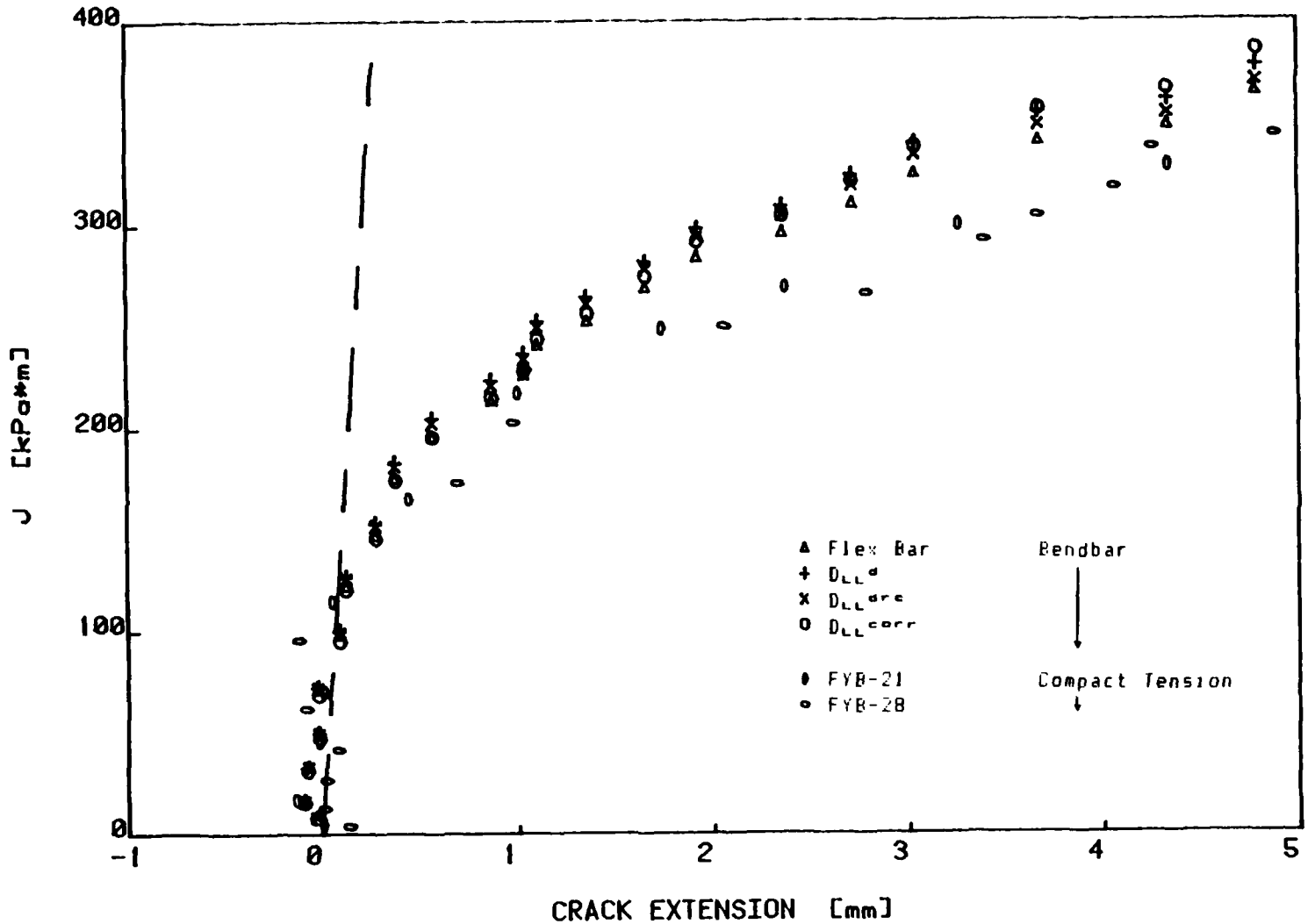


Figure 15b - J-R Curves for 3-Ni Bendbar FYB-511 With Different Load Line Deflection Measurements Compared to Data from Two Compact Tension Specimens of 3-Ni Steel

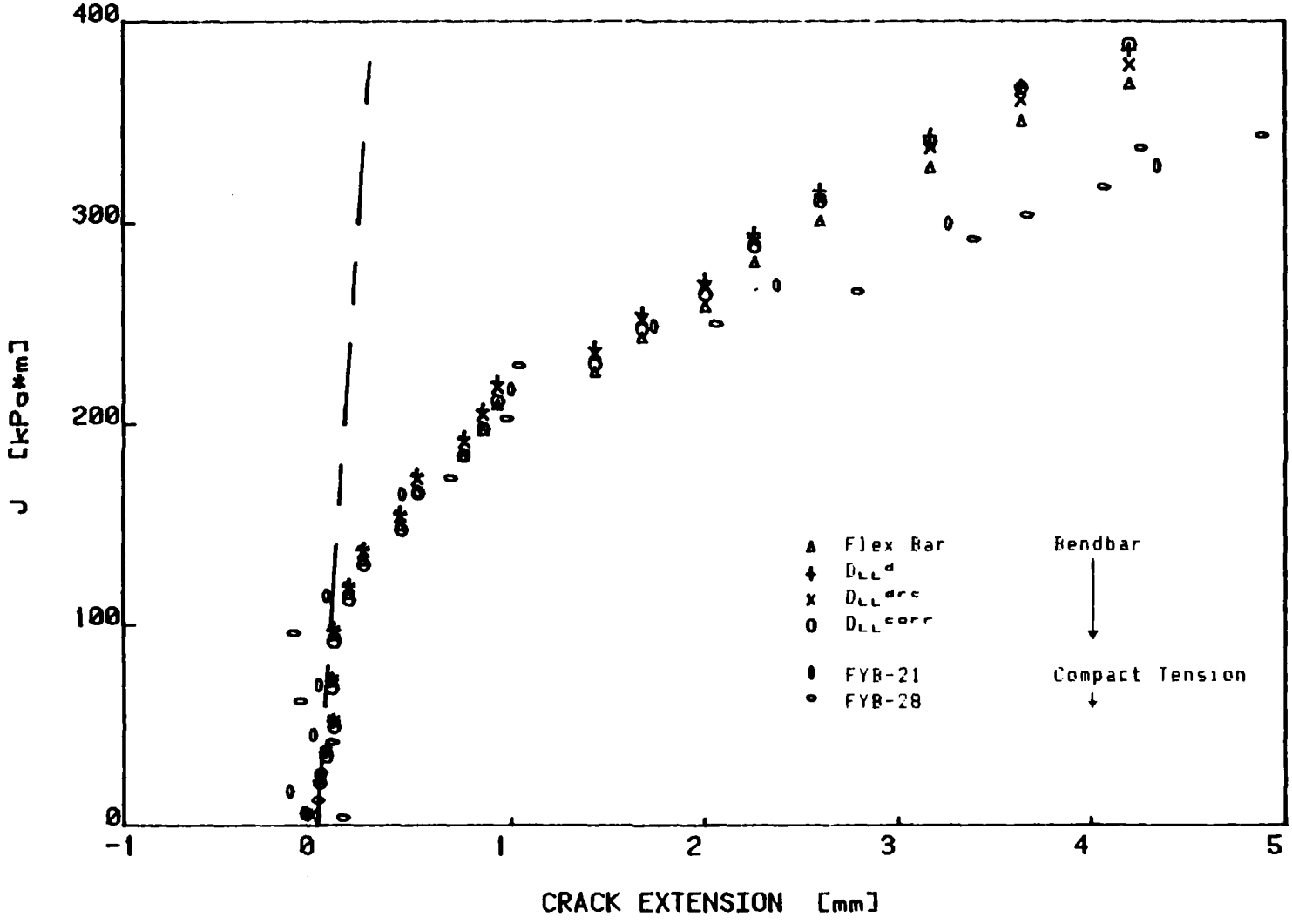


Figure 15c - J-R Curves for 3-NI Bendbar FYB-512 with Different Load Line Deflection Measurements Compared to Data from Two Compact Tension Specimens of 3-NI Steel

## REFERENCES


1. Gudas, J.P. and D.A. Davis, "Evaluation of the Tentative $J_1$-R Curve Testing Procedure by Round Robin Tests of HY130 Steel," Journal of Testing and Evaluation, JETVA, Vol. 10, No. 6, pp. 252-262 (Nov 1982).

2. Joyce, J.A. and E.M. Hackett, "Dynamic J-R Curve Testing of 3-Ni Steel Using the Key Curve and Multi-Specimen Techniques," Presented at the ASTM 17th National Symposium on Fracture Mechanics, Albany, N.Y. (July 1984).

3. Albrecht, P., et al, "Tentative Test Procedure for Determining the Plane Strain J-R Curve," Journal of Testing and Evaluation, JETVA, Vol. 10, No. 6, pp. 245-251 (Nov 1982).

4. Wells, A.A. in Proceedings, Canadian Congress of Applied Mechanics, Calgary, Alta., Canada pp. 59-77 (1971).

5. Garwood, S.J., "The Effect of Specimen Geometry on the Crack Growth Resistance of API 5LX65 Steel," The Welding Institute, Report 61/1978/E

6. Joyce, J.A. and J.P. Gudas, "Computer Interactive $J_{IC}$ Testing of Navy Alloys," ASTM STP 668, American Society for Testing and Materials, pp. 451-468 (1979).

## INITIAL DISTRIBUTION

| Copies | |
|---|---|
| 1 | ONR Code 471 |
| 1 | NAVMAT 034 |
| 4 | NRL |
| | 1 Code 6000 |
| | 1 Code 6380 |
| | 1 Code 6320 |
| | 1 Code 6396 |
| 10 | NAVSEA |
| | 1 SEA 05D |
| | 1 SEA 05R |
| | 1 SEA 08 |
| | 1 SEA 092 |
| | 1 SEA 323 |
| | 1 SEA 393 |
| | 1 SEA 395 |
| | 1 SEA 396 |
| | 2 SEA 99612 |
| 1 | NISC Code 369 |
| 12 | DTIC |

CENTER DISTRIBUTION

| Copies | Code | |
|---|---|---|
| 1 | 17 | Krenzke |
| 1 | 1720.1 | Kiernan |
| 1 | 28 | |
| 1 | 2801 | Crisci |
| 5 | 281 | Wacker |
| 4 | 2813 | Morton |
| 10 | 2814 | Gudas |
| 15 | 2814 | Kirk |
| 1 | 522.1 | TIC |
| 2 | 5231 | Office Services |

DTNSRDC ISSUES THREE TYPES OF REPORTS

1. DTNSRDC REPORTS, A FORMAL SERIES, CONTAIN INFORMATION OF PERMANENT TECHNICAL VALUE. THEY CARRY A CONSECUTIVE NUMERICAL IDENTIFICATION REGARDLESS OF THEIR CLASSIFICATION OR THE ORIGINATING DEPARTMENT.

2. DEPARTMENTAL REPORTS, A SEMIFORMAL SERIES, CONTAIN INFORMATION OF A PRELIMINARY, TEMPORARY, OR PROPRIETARY NATURE OR OF LIMITED INTEREST OR SIGNIFICANCE. THEY CARRY A DEPARTMENTAL ALPHANUMERICAL IDENTIFICATION.

3. TECHNICAL MEMORANDA, AN INFORMAL SERIES, CONTAIN TECHNICAL DOCUMENTATION OF LIMITED USE AND INTEREST. THEY ARE PRIMARILY WORKING PAPERS INTENDED FOR INTERNAL USE. THEY CARRY AN IDENTIFYING NUMBER WHICH INDICATES THEIR TYPE AND THE NUMERICAL CODE OF THE ORIGINATING DEPARTMENT. ANY DISTRIBUTION OUTSIDE DTNSRDC MUST BE APPROVED BY THE HEAD OF THE ORIGINATING DEPARTMENT ON A CASE BY CASE BASIS.

END

FILMED

3-86

DTIC